重要用語に対するQ8とQ10の共同作業を行うことです．四つ目はModule 3の重要事項，エッセンスを盛り込んだQOSを作りたいとの意見もありますので，それに関する改定指針の作成を検討することです．五つ目は科学の技術の進歩を反映した既存ガイドラインの見直しの是非を検討することです．これらは課題提起であり，合意されたものではありません．

その他，企業は大いに関心のある重要事項として考えていますが，規制側はそれによって影響を受けるとの理由で消極的である事項との前提つきで，市販後の変更管理システムが調和していないことも企業側から問題点として挙げられました．更に，承認申請とライフサイクルに関する部分と区別してアプリケーションする仕組みができないかといったこともEFPIA，PhRMAから提案されました．

8. Proposed Next Steps (Table 23)

次のステップへの計画については，Table 23に示していますが，この一つ目はグループに諮ることなく，世話役が独断で作成したものをSCで発表したものです．しかし，SCがこのまま是認してしまいました．先ほどから問題となっているQuality Strategyについての調和とその作業計画に関する議論を続け，次回のブリュッセル会議で終わりにする予定としているということです．「終わりにする」という言葉が何を意図しているかにもよりますが，「統一化を遂げるという終わりにする」という意図の可能性も大いにありですので，今後の対応について頭の痛い問題です．

また，原薬ガイドラインに関して化成品とバイオの専門家が対話をすること，これは合意したことです．

Table 23　Proposed Next Steps

- The two co-chairs suggest
  - To continue and finalise ICH Q strategy discussion in Brussels in order to work out a harmonised quality strategy and a workplan.
  - To continue the dialogue between chemical experts and biotech experts on a section S2 (drug substance) guideline.

9. 今後に向けて

9.1 現状分析

品質に関してはCTD Module 3，GMPなどをベースにR&D，あるいは承認申請，審査，製造販売承認，市販後対応をしてきた欧米は，産・官とも合理化，効率化を目指すと共に，新たな品質概念やシステムを導入した域内でのパラダイムシフトを図ろうとしています．そうした動きの中核をなす概念や方策が，QbD，DS，QRM，Life cycle approachなどで，これに関連したICHガイドラインがQ8，Q9，Q10です．特に欧米の企業は世界戦略，EUは域内統合，FDAは最近確定した新しい薬事行政路線の展開の観点などから，これらがICHレベルで浸透することを推進しようとしています．シカゴ会議は，こうしたヴィジョンの三極での合意と達成のための戦略，行動計画の策定を目指したものでした．

FDAは，Q8，Q9，Q10の施行結果を見極めてから次の行動を取りたいとしています．

EUは，現時点ではICHレベルでの品質戦略活動に関してFDAより積極的な方向に転じたように見えます．しかし，ICHが規制当局を縛るべきではないと考える側面も持ち合わせているようにも見えます．

欧米の企業は，世界同一規制の実現を最終目標に，前進を図る考えです．Q8の一部，Q9，Q10はオプションとして示されていますが，欧米の産・官にとっては品質戦略の中核となります．その認識に立ってICHレベルで議論しようとしているところに彼我の大きなギャップがあるように思います．

9.2 論点の再整理

以上述べてきましたことの論点を，科学面，ガイドライン面，規制面，調和活動面から再整理してみたいと思います．

9.2.1　科学面

品質課題の最終目的は，有効性，安全性の確保にあり，品質確保はその手段です．品質自体（手段）を目的とした品質論（自己目的化）は一義的目標ではなく，基本的概念にもなり得ないと思います．

また，品質確保にはさまざまな科学的方策があり，製品の特性，規制環境，企業の創意工夫などといったそれぞれの状況に応じて適用され，目的を達することができればそれで良いと思います．ICHはそれらの科学的要素や方策・手段を提供する方針をと

ってきました．最近は概念，方策及びシステムの一元化を図るような動きが顕著です．これらがオプションや参考事項に止まっているうちは有用ですが，一元化やその強制化は必ずしも適切ではないと思います，科学的な創造活動と方策を一元化することは，そもそも二律背反する要素です．

9.2.2　ガイドライン面

ガイドライン面では，Q9は現行の規制要件を越えた新たな要件を創出することは意図しないとガイドラインに記載されています．また，Q10はオプション，Q8は製剤開発に関するガイドラインで，“Design Space”は選択肢の一つとされています．

そういった位置づけのものが今後のICHガイドライン作成の基盤要件，前提条件のごとく関係付けられ，また既存のガイドラインの見直しの根拠になることは，論理的にも規制的にも適切でありません．

“Quality by Design”，“Design Space”などの用語や概念には，極めて多様な解釈や理解があり，状況によって多様な適用の仕方があります．そうした用語を上位概念的にすべてのICH-Qガイドラインに適用することは問題が多く，品質の最上位概念とも言えません．内容的に同一趣旨のことは，その状況や必要に応じ，一般的用語で適切に既存のICHガイドラインに既に述べられてきています．必要な概念を言いたいのであれば，適宜，その状況に応じて内容を平易に説明する方が良いと思われます．一つの言葉で括ろうとすることにはいろいろ無理があります．

“QRM”や“Life cycle approach”など，全体方策やシステムに関わるQ9，Q10を他のガイドライン作りのベース，あるいは前提条件の一つとして仮に位置付けるとしますと，例えば製造方法に関する新たなガイドラインを作成して施行した時点でそのガイドライン自体は拘束力を持ちますので，そのガイドラインを介してオプションであるはずのQ9やQ10の関連する内容が結果的に新たな規制要件，拘束力を創り出すこととなります．

“QRM”や“Life cycle approach”は，その本質から見て，新薬のみならず，あらゆる医薬品に適用しなければ政策的，概念的整合性がとれない，という側面を持っています．拘束力を持つ規制要件となりますと，日本国内の医薬品規制に重大な影響を及ぼすため，大きな問題になると思われます．

MHLWは，Q9及びQ10による新たな規制システムや方策を整備するということ，あるいは現行規制がQ9及びQ10により影響を受けることは意図していないとしています．仮に良い考えであったとしても，現実対応が困難であり，現行規制を順守すれば必要な品質確保は可能であるのにわざわざそこまでする必要はないということです．

9.2.3　規制面

品質，特に製法の取り扱い問題は各極の承認事項や承認制度の根幹に触れる側面を持つことをきちんと認識，整理しておく必要があります．日本が欧米の動きにどこまで歩調を合わせるか，もしくは合わせざるかを国益，国際益のバランスシートにかけて対応する必要があります．

CTD Module 3のエッセンスをQOSに，QOSのエッセンスを承認事項としてきた日本の承認制度や承認書は，リソースに乏しい日本で工夫された合理性の極致と言えます．QOSの合理性，効率性が見直されているということは，その表れであり，欧米が目指している様々な政策の一つのあり方が，実は日本にあるのではないかと考えられます．こういった優れた方策に更に磨きをかける視点で対応すれば良いのではないかと思っています．

9.2.4　調和活動面

目標達成のため，各極関係者がとる方策，手段はそれぞれの実状，合理性，効率性に合ったフレキシブルなものであるべきであり，制度やシステムの変更に及ぶような合意への要請は，国際調和活動とは言えないと思います．

ICH調和文書では，その目的から見て，用語，概念，文章などが共通の理解や解釈をもたらすことが生命線であり，それらに相違ができれば，調和文書から非調和が生まれるということになります．これを回避するために，全ての関係者に共通の理解や解釈をもたらす平易で明快な用語や概念を用いてガイドラインを作成すべきと思います．欧米人にさえ難解な英語を無理に理解させようとするのは調和活動とは言えません．現在のような概念論争でICHガイドラインの作成が遅延していくのはICHの精神にも公益にも反すると思います．

ICHガイドラインには1）各極に共通のニーズ，目標が存在すること，2）その背景となる基本概念，目標達成に必要な科学的原則や要素，普遍的な方

策・手段に関する議論が同一基盤で成り立つこと，3）成果が各極，各関係者に受入れられ，共有され，活用されることなどの要件が重要です．

これらの要件が充たされる程度がより高いほど，ICH ガイドライン作成の意義はより高くなりますので，今後の推移を見ながら適切に対応をしていかなければならないと思います．

Available online at www.sciencedirect.com
ScienceDirect
Biochemical and Biophysical Research Communications 356 (2007) 1024–1030
BBRC
www.elsevier.com/locate/ybbrc

Induction of human adiponectin gene transcription by telmisartan, angiotensin receptor blocker, independently on PPAR-γ activation

Akie Moriuchi [a,b], Hironori Yamasaki [a,c,*], Mika Shimamura [d], Atsushi Kita [a], Hironaga Kuwahara [a], Keiichiro Fujishima [a,b], Tsuyoshi Satoh [a], Keiko Fukushima [a,b], Tetsuya Fukushima [a], Takao Hayakawa [e], Hiroyuki Mizuguchi [e], Yuji Nagayama [f], Norio Abiru [a], Eiji Kawasaki [b], Katsumi Eguchi [a]

[a] *Department of Endocrinology and Metabolism, Unit of Translational Medicine, Graduate School of Biomedical Science, Nagasaki University, Japan*
[b] *Department of Metabolism/Diabetes and Clinical Nutrition, Nagasaki University, Hospital of Medicine and Dentistry, Nagasaki, Japan*
[c] *Health Center, Nagasaki University, Japan*
[d] *Course of Pharmaceutical Sciences, Graduate School of Biomedical Science, Nagasaki University, Japan*
[e] *Project III, National Institute of Health Sciences, Osaka Branch, Fundamental Research Laboratories for Development of Medicine, Japan*
[f] *Department of Medical Gene Technology, Atomic Bomb Disease Institute, Graduate School of Biochemical Sciences, Nagasaki University, Japan*

Received 14 March 2007
Available online 26 March 2007

Abstract

Adiponectin, an adipose tissue-specific plasma protein, has been shown to ameliorate insulin resistance and inhibit the process of atherosclerosis. Recently, several reports have stated that angiotensin type 1 receptor blockers (ARBs), increase adiponectin plasma level, and ameliorate insulin resistance. Telmisartan, a subclass of ARBs, has been shown to be a partial agonist of the peroxisome proliferator-activated receptor (PPAR)-γ, and to increase the plasma adiponectin level. However, the transcriptional regulation of the human adiponectin gene by telmisartan has not been determined yet. To elucidate the effect of telmisartan on adiponectin, the stimulatory regulation of human adiponectin gene by telmisartan was investigated in 3T3-L1 adipocytes, utilizing adenovirus-mediated luciferase reporter gene-transferring technique. This study indicates that telmisartan may stimulate adiponectin transcription independent of PPAR-γ.

Keywords: Adiponectin; Telmisartan; PPAR-γ

Adiponectin has been shown to improve insulin sensitivity and inhibit the process of atherosclerosis [1]. Recently, a metabolic syndrome characterized by an excess accumulation of visceral fat associated with insulin resistance and leading to atherosclerotic vascular events has been on the increase. However, these patients exhibit the lower plasma concentration of adiponectin [2,3]. Weight gain with visceral fat accumulation, is associated with a decrease in mRNA expression and plasma level of adiponectin [4–6]. Tumor necrosis factor-α, proinflammatory cytokine secreted from adipocytes suppressed adiponectin expression and secretion [7–9]. In contrast, reducing body weight by diet and exercise therapy stimulates an increase in adiponectin concentration [10,11]. Recently the anti-diabetic drug thiazolidinediones, an insulin sensitizer, has been shown to increase adipocytes mRNA expression of adiponectin and plasma concentration [9,12]. Several years ago, the human adiponectin promoter sequence was cloned, and analyzed to identify the critical responsive element for transcriptional regulation [13,14]. Peroxisome proliferator-activated receptor (PPAR)-γ has been shown to play an important role in the up-regulation of adiponectin expression [15]. Recently, a number of reports have been published which indicate that angiotensin II type 1

* Corresponding author.
E-mail address: f1195@cc.nagasaki-u-ac.jp (H. Yamasaki).

0006-291X/$ - see front matter © 2007 Elsevier Inc. All rights reserved.
doi:10.1016/j.bbrc.2007.03.084

receptor (AT1R) blockers (ARBs), commonly used to treat hypertension, reduced insulin resistance [16,17], lowered the risk for type 2 diabetes [18,19] and, increased the plasma level of adiponectin [17,20,21]. Telmisartan, a subclass of ARBs has been reported to associate with PPAR-γ as a partial agonist [22,23]. These observations allowed the speculation that telmisartan could stimulate adiponectin via PPAR-γ. Therefore, the transcriptional regulation of human adiponectin by telmisartan in 3T3-L1 adipocytes was examined. In order to increase the assay sensitivity, an adenovirus-mediated luciferase reporter vector containing human adiponectin 2.1 kb promoter region was created.

Materials and methods

Materials. Pioglitazone and candesartan were kindly provided by Takeda Pharmaceutical Company (Osaka, Japan), Telmisartan by Boehringer Ingelheim (Ingelheim, Germany). PD98059 and LY294002 were purchased from Cell Signaling Technology (Beverly, MA), GW9662 from CALBIOCHEM (Darmstadt, Germany).

Isolation of human adiponectin promoter and luciferase construct (pAdp-LUC. The 5′ product of the human adiponectin gene, spanning 2.1 kb of the genomic sequence, was amplified [24], and subcloned into PGL3-Basic Vector. The resultant luciferase reporter construct was designated pAdp-LUC as previously described [8].

Modification of the shuttle vector and adenoviral vectors. A pHMCMV6 is a shuttle vector for constructing adenoviral vectors [25]. In order to evaluate the promoter activity by adenoviral vectors, a modification was made in pHMCMV6. A sequence-including CMV promoter multiple cloning sites, and a polyA region were deleted from pHMCMV6 by digesting pHMCMV6 with *Bgl*II (*Bgl*II-*Bgl*II-pHMCMV6). By digesting pGL3-Basic Vector with *Not*I and *Bam*HI, the 2.1 kb fragment was excised; this fragment included multiple cloning sites and luciferase coding and PolyA regions. This fragment and *Bgl*II-*Bgl*II-pHMCMV6 were blunted and ligated to provide an original shuttle vector for an adenoviral-mediated luciferase reporter. The resultant plasmid was designated p0-LUC-Shuttle.

A 2.1 kb promoter fragment subcloned into p0-LUC-Shuttle. The resultant plasmid, pAdp-LUC-Shuttle, was then digested with I-*Ceu*I and PI-*Sce*I and ligated into an adenoviral vector, pAdHM15 [26]. This resultant adenoviral DNA, fmAd-pAdp-LUC, provides for luciferase reporter expression regulated by the human adiponectin promoter, illustrated in Fig. 1A. An fmAd-pAdp-LUC was linealized with *Pac*I and transfected into HEK293 cells to produce the adenoviruses, fmAd-pAdp-LUC.

In order to verify PPAR-γ activity, luciferase reporter vector driven by PPAR responsive element (PPRE) was prepared. TransLucent Reporter Vectors containing PPAR responsive element (PPRE, 3 time tandem repeat of TGAAACTAGGGTAAAGTTCA, from Panomics (Fremont, CA), and this tandem repeat was subcloned into p0-LUC-Shuttle, designated PPRE-LUC.

A Renilla luciferase-expression adenovirus vector was also prepared to serve as an internal control. By digesting with *Bgl*II and *Bam*HI, a 2.2-kb fragment was excised from phRLTK-Vector (Promega). This fragment and *Bgl*II-*Bgl*II-pHMCMV6 were blunted and ligated (phRLTK-LUC-Shuttle). Then, as described above, control adenoirus was created, designated fmAd-phRLTK-LUC.

Cell culture and infection with adenovirus. 3T3-L1 preadipocytes purchased from ATCC were differentiated according to previously described

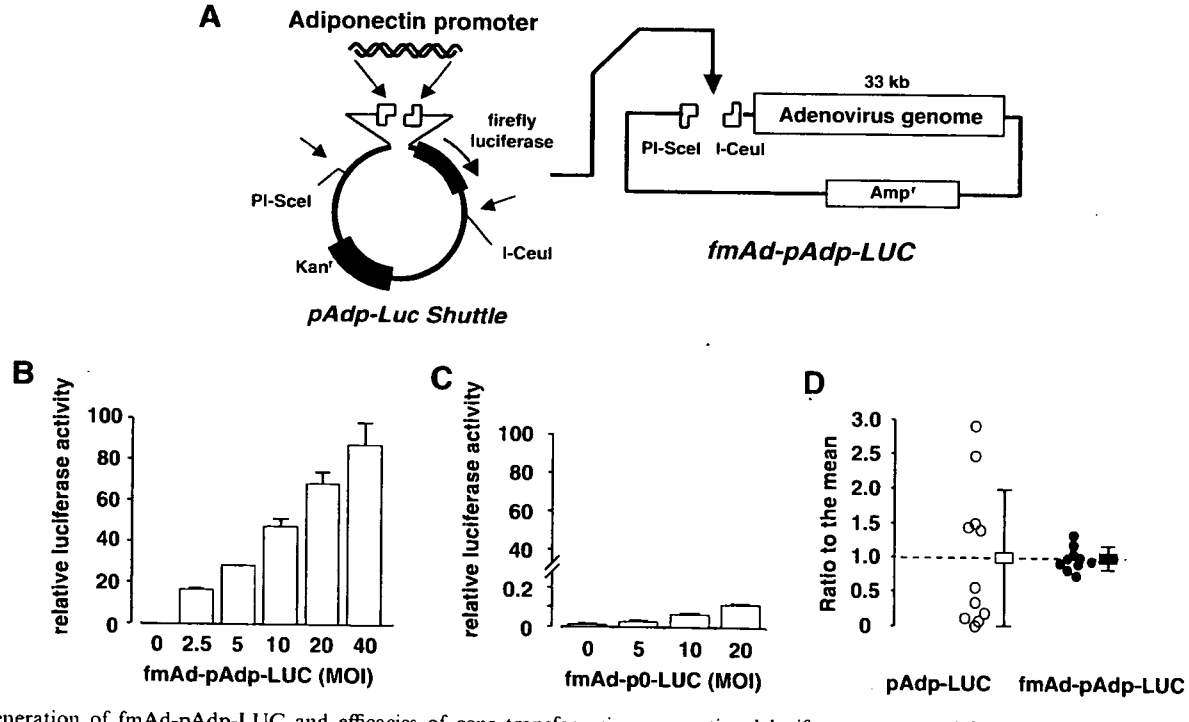

Fig. 1. Generation of fmAd-pAdp-LUC and efficacies of gene transfer using conventional luciferase vector (pAdp-LUC) and adenovirus-mediated luciferase vector (fmAd-pAdp-LUC) in 3T3-L1 adipocytes. (A) The 2.1 kb human adiponectin promoter was subcloned into the shuttle vector to drive firefly luciferase. This promoter-luciferase unit was excised and subjected to in vitro ligation to adenovirus vector (fmAd-pAdp-LUC). (B,C) 10 MOI of fmAd-pAdp-LUC (B) or 10 MOI of fmAd-p0-LUC (C) were infected into 3T3-L1 adipocytes. After 3 h of infection, cells were incubated for another 24 h. Cells were lysed and assayed using the luciferase assay. Results are expressed as relative light unit of firefly luciferase. Each bar represents mean ± SD ($n = 3$). (D) 2 μg/well of pAdp-LUC and 10 MOI of fmAd-pAdp-LUC were infected. Each plot is expressed as a ratio to the mean, which was adjusted to 1.

methods [27]. Fully differentiated 3T3-L1 adipocytes were transfected with fmAd-pAdp-LUC with an adenovirus concentration of 10 MOI.

Transient transfection with the plasmid of PPRE-LUC. HEK293 cells were transiently transfected with 500 ng/well of PPRE-LUC, 600 ng/well of pCMV6-PPAR-γ2 kindly provided by Ogawa MD (Kobe University) and 20 ng/well of phSV40 as an internal control. Transient transfection was done by SuperFect Transfection Reagent, purchased from QIAGEN.

Luciferase assay. The luciferase activitiy was measured using the Dual-Luciferase Reporter Assay System (Promega) and Turner Designs Luminometer model TD-20/20 (Promega).

Statistical analysis. Differences in the luciferase activity were assessed by unpaired *t* testing. *p* values less than 0.05 were considered to be statistically significant.

Results

Construction of adenovirus-mediated luciferase reporter vector and its functional property in 3T3-L1 adipocytes

Due to the low transfection efficiency of 3T3-L1 adipocytes using conventional method of transfection, an adenovirus-mediated luciferase reporter vector was created, in which the luciferase gene was driven by the human adiponectin promoter. The resultant adenovirus, fmAd-pAdp-LUC, was infected into 3T3-L1 adipocytes. The luciferase activity was detected in the fmAd-pAdp-LUC-infected cells in a dose-dependent manner (Fig. 1B). However, negligible luciferase activity was detected in the cells infected with promoter-less adenovirus vectors, designated fmAd-p0-LUC (Fig. 1C). Furthermore, the pAd-LUC to fmAd-pAd-LUC was compared, with regard to reproducibility of luciferase assay. The luciferase activity from fmAd-pAdp-LUC infection was more consistant than that from pAdp-LUC vector transfection (Fig. 1D). These data suggest that fmAd-pAdp-LUC facilitates sensitive and reproducible analysis of the promoter activity in 3T3-L1 adipocytes.

Telmisartan stimulated the human adiponectin transcription as well as pioglitazone

A culture of fmAd-pAdp-LUC-infected 3T3-L1 adipocytes were treated with 10 μM pioglitazone and increasing concentrations of telmisartan. Fig. 2A demonstrates that adiponectin promoter activity was stimulated at 2.9-fold by 10 μM pioglitazone, which was sufficient for maximal stimulation of adiponectin transcription (data of dose-dependent experiment is not shown). The promoter activity was stimulated by telmisartan in a dose-dependent manner, up to 5 μM. The maximal stimulation was 2.1-fold, which was lower than that of 10 μM pioglitazone. The promoter activity was appeared to decline when exposed to >10 μM telmisartan. This could suggest that high concentration of the drug has a toxic effect. In determine if this stimulation was specific to telmisartan, candesartan, the other subclass of ARBs, was used (Fig. 2B). In contrast to telmisartan, candesartan induced no significant alteration, even at the higher concentrations.

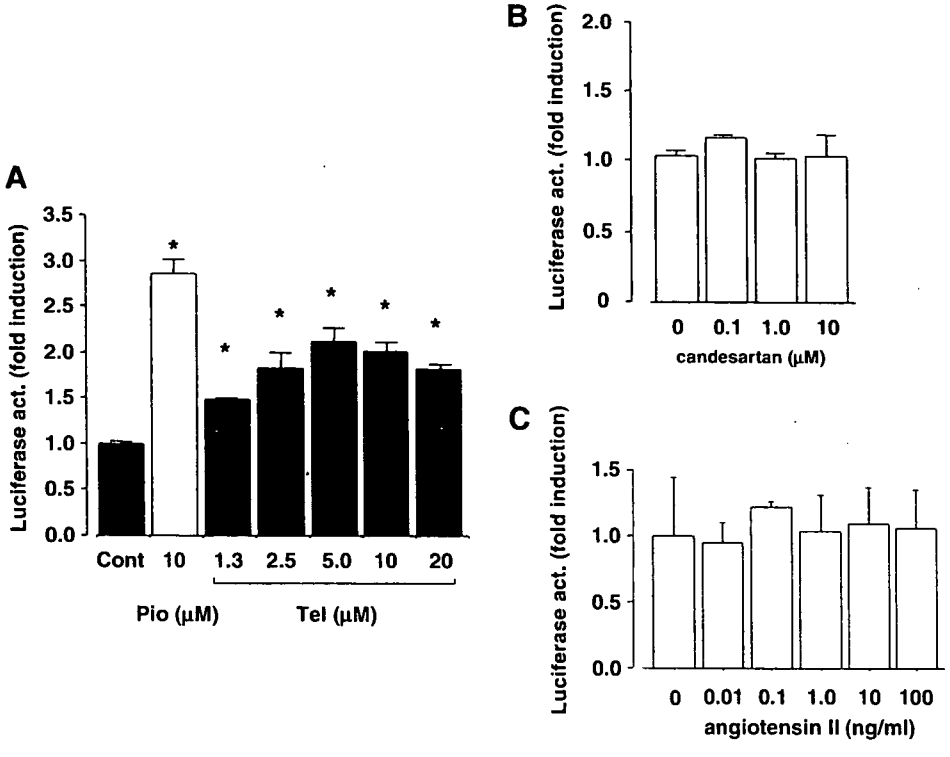

Fig. 2. Effect of pioglitazone, candesartan, telmisartan and angiotensin II on adiponectin transcription. Cells were infected with fmAd-pAdp-LUC, stimulated by Pio (pioglitazone), Tel (telmisartan) (A), candesartan (B) and angiotensin II (C). After 24 h, cells were assayed using the luciferase assay. Results are expressed as fold induction compared to control. Each bar is mean ± SD ($n = 3$). $^*p < 0.05$ basal versus treatment.

Angiotensin II did not regulate adiponectin transcription

Since telmisartan essentially blocks the angiotensin II receptor, it is important to investigate the association of angiotensin II receptor activation with adiponectin transcription.

Presuming that angiotensin II receptor activation by angiotensin II supresses adiponectin transcription then blocking of the receptor by telmisartan could have restored the suppressed transcription. Fig. 2C demonstrates that the angiotensin II neither suppressed nor stimulated the adiponectin transcription. These data suggest that telmisartan's stimulatory activity is evoked via a mechanism independent of the receptor.

MAP kinase pathway and PI-3 kinase pathway did not meditate the telmisartan's stimulation of adiponectin transcription

To investigate the contribution of insulin signaling pathways to telmisartan's stimulation, inhibitors of MEK and PI3 kinase were employed. Neither MEK inhibitor, PD98059 nor PI3 kinase inhibitor, LY294002 could prevent the stimulation by telmisartan shown in (Fig. 3A and B). These data indicate that neither the MAP kinase nor PI3 kinase pathways contribute to the stimulatory effect of telmisartan.

Telmisartan-stimulated adiponectin transcription is independent of PPAR-γ activation

Recently, telmisartan has been reported to be a partial agonist to PPAR-γ. In addition, a PPAR responsive element (PPRE) is present on the human adiponectin promoter sequence. However, there is no evidence that the telmisartan's stimulatory effect of adiponectin transcription is mediated by PPAR-γ. To investigate the role of PPAR-γ in the telmisartan activity, fmAd-pAdp-LUC-infected 3T3-L1 adipocytes were cultured with or without PPAR-γ inhibitor, GW9662, and incubated with pioglitazone and telmisartan. The stimulation by pioglitazone was completely blunted by GW9662 pretreatment (Fig. 4A). In contrast, the stimulation by telmisartan was still observed even with GW9662 pretreatment. These data suggest that the telmisartan's stimulation of adiponectin is independent of PPAR-γ regulation.

PPAR-γ responsive element (PPRE) is stimulated by both pioglitazone and telmisartan

The ability of telmisartan to stimulate PPAR-γ was also investigated using PPRE-LUC. PPRE-LUC-transfected HEK293 cells were cultured with or without GW9662 and incubated with pioglitazone and telmisartan. Fig. 4B shows that the transactivation of PPRE was induced 3.3-fold by 10 μM pioglitazone and 1.6-fold by 5 μM telmisartan. Pretreatment with GW9662 completely blocked the transactivation of PPRE by both drugs. This indicates that telmisartan is apparently a PPAR-γ agonist, although the stimulatory activity was lower than with pioglitazone. In addition, the observation that GW9662 blocks the telmisartan stimulation of PPAR-γ, confirms the fact that telmisartan stimulates PPAR-γ.

Discussion

In this study, human adiponectin gene transcription was analyzed in 3T3-L1 adipocytes, utilizing an adenovirus-mediated luciferase reporter gene-transferring technique. Adiponectin transcription was stimulated by pioglitazone as well as telmisartan. Furthermore, the inhibitor experiments showed that the pioglitazone's effect was PPAR-γ-

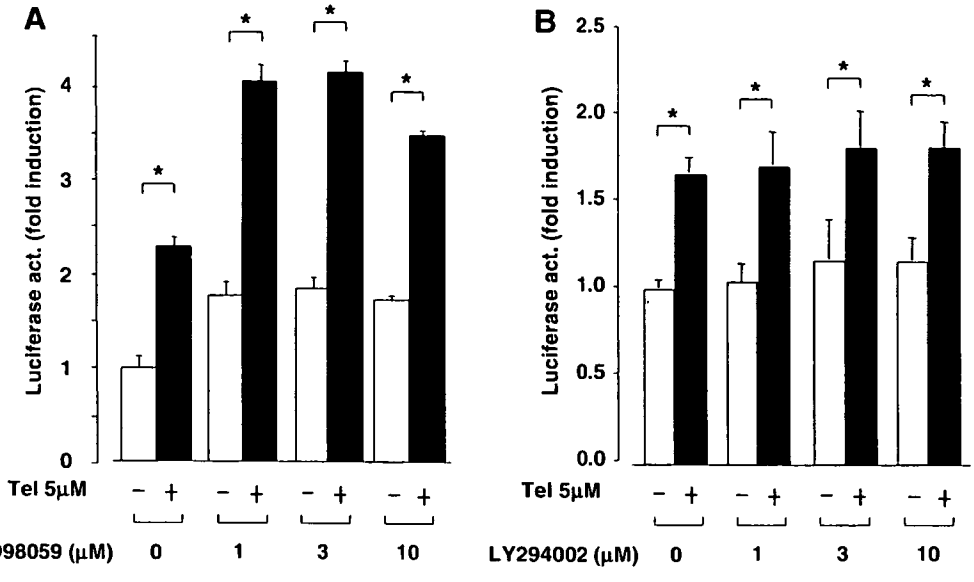

Fig. 3. Effects of inhibitors of MAP kinase and PI3 kinase on telmisartan-induced stimulation of adiponectin. Cells were infected with fmAd-pAdp-LUC, followed by 1 h incubation with PD98059 (A) or LY 294002 (B). Then, cells were treated with telmisartan. Results are expressed as fold induction over each untreated group. Each bar is mean ± SD ($n = 3$). *$p < 0.05$ basal versus treatment at each concentration of inhibitor.

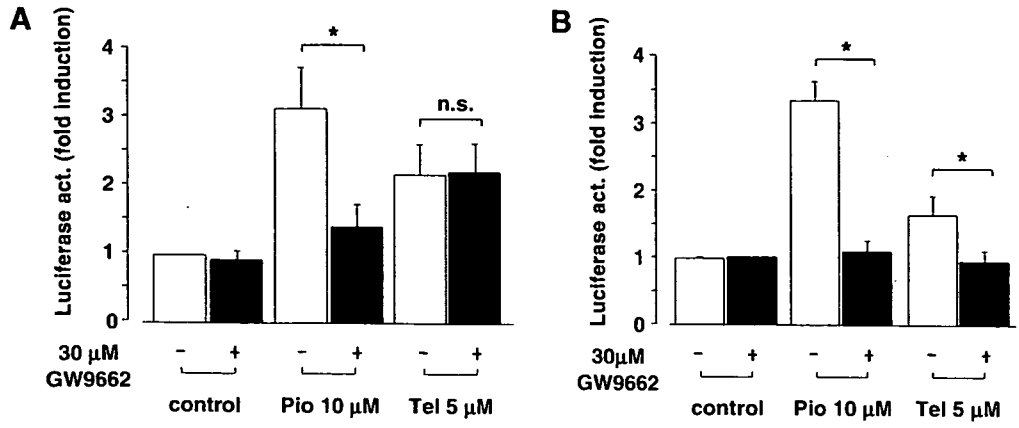

Fig. 4. Effect of PPAR-γ inhibition on pioglitazone- and telmisartan-induced stimulation of adiponectin and PPAR-γ. (A) 3T3-L1 adipocytes were infected with fmAd-pAdp-LUC followed by pretreatment with GW9662 for 1 h. (B) HEK 293 cells were transiently co-transfected with fmAd-PPRE-LUC and CMV6-PPAR-γ2 together with phSV40-LUC as an internal control for 3 h. Results are expressed as fold induction over the untreated group. Each bar is mean ± SD from four independent experiments. $^{*}p < 0.05$, GW9662 treatment versus untreatment.

dependent, while the telmisartan's effect was PPAR-γ-independent.

PPAR-γ has shown to be a master regulator for adipocyte differentiation. Attenuating PPAR-γ expression and activity result in impaired adipocyte differentiation [28–30]. Activation of PPAR-γ is required for the expression of adipocyte-specific markers, including fatty acid binding protein 3, GLUT 4, insulin receptors, insulin receptor substrate (IRS), and C/EBPα [30,31]. The adiponectin gene is also adipocyte-specific, and the expression of this gene increases with adipocyte differentiation. Several groups have investigated the transcriptional regulation of adiponectin, showing that SP1/SP3 [13], SREBP-1c [14] and C/EBP-β [8] are crucial transcription factors for constitutive or ligand-dependent expression. Osaka University has recently identified a PPAR-γ responsive element in the region −285 to −273 (5′-TGACTTTTGCCCC-3′) in the adiponectin gene, and demonstrated that mutation of that sequence abolishes pioglitazone-induced stimulation of adiponectin transcription [15]. These data suggest that the elevation of serum adiponectin concentration, observed in clinical use of pioglitazone, may in part, resulted from transcriptional regulation. The assay system used in this study also demonstrated that adiponectin transcription is directly stimulated via PPAR-γ activation (Fig. 4A). Interestingly, under basal conditions (absence of pioglitazone), pretreatment with a PPAR-γ inhibitor do not change the level of adiponectin transcription. These data suggest that basal transcriptional activity is dependendent upon transcription factors other than PPAR-γ.

Recent studies have demonstrated that telmisartan act as a partial agonist of PPAR-γ [22,23]. It has been suggested that telmisartan-bound PPAR-γ shows conformational change different to that elicited by rosiglitazone [32]. The present study produced similar data by utilizing a reporter vector containing PPAR-γ consensus sequences (Fig. 4B). Treatment with telmisartan increased the PPAR-γ activity, and that stimulation was blocked a by PPAR-γ inhibitor, GW9662. Surprisingly, that pretreatment with PPAR-γ inhibitor failed to prevent telmisartan's stimulatory effect on adiponectin transcription (Fig. 4A). These data suggest that telmisartan enhances the adiponectin transcription, independent of PPAR-γ activation.

Induction of PPAR-γ-dependent gene expression by telmisartan has been recently studied on RAGE mRNA. Telmisartan suppressed RAGE protein synthesis in Hep3B cells, and this was blocked by PPAR-γ inhibitor, GW9662 [33]. If telmisartan, like pioglitazone acts only as a PPAR-γ agonist, identical regulation of gene expression should be observed with all PPAR-γ-target genes. Micro-array analysis, however, shows that the gene expression profiles induced by pioglitazone and by telmisartan are not the same [32], suggesting that telmisartan may have a different signaling mechanism than pioglitazone.

The results presented here demonstrated that adiponectin transcription showed PPAR-γ-dependence when it was stimulated by pioglitazone, not by telmisartan. Why has adiponectin transcription developed PPAR-γ-independence? There are possible explanations that would account for these results. First, it is possible that the PPAR-γ inhibitor, GW9662 concentration used in this study was too small to sufficiently inhibit the effect of telmisartan. This is, however, unlikely because the same concentration of GW9662 almost completely inhibited PPAR-γ activation by telmisartan (Fig. 4B). Second, telmisartan-bound PPAR-γ may not be associated with the PPAR-γ responsive element on the human adiponectin promoter that was identified by Iwaki et al. [15]. If not, telmisartan may activate other known or unknown transcription factor(s) which regulate the human adiponectin transcription. There are two reasons why telmisartan-activated PPAR-γ does not associate with PPAR-γ responsive element on human adiponectin promoter. The sequence previously reported shows little homology to the PPAR-γ consensus sequence, and is located on an anti-sense strand of the gene. Binding of telmisartan to PPAR-γ may result in a different protein

configuration than that resulting from the binding of pioglitazone. This three-dimensional change in protein configuration may prevent the association of PPAR-γ with the PPAR-γ responsive element previously reported.

What do stimulatory effects of telmisartan depend on? It is postulated that telmisartan may bind and activate PPAR-α. PPAR-α is expected to be a crucial transcriptional factor for adiponectin gene expression, because in the assay system used in this study bezafibrate, a PPAR-α agonist, was found to stimulate adiponectin transcription (data not shown). It has also been reported that administration of bezafibrate increased both the mRNA and plasma level of adiponectin [34,35].

The present study indicates that telmisartan stimulates adiponectin transcription by a PPAR-γ independent mechanism. Identification of this mechanism, could lead to the development of a new drug for hypoadiponectinemia, which is commonly seen in metabolic syndrome and type 2 diabetes. Precise understanding of this molecular mechanism will require further investigation.

Acknowledgments

The authors thank Miss. Ayako Kaneko for her excellent technical assistance. This work was supported by a grant from Metabolic Syndrome Research Conference in Kyushu to H.Y.

References

[1] T. Kadowaki, T. Yamauchi, N. Kubota, K. Hara, K. Ueki, K. Tobe, Adiponectin and adiponectin receptors in insulin resistance, diabetes, and the metabolic syndrome, J. Clin. Invest. 116 (2006) 1784–1792.

[2] M. Ryo, T. Nakamura, S. Kihara, M. Kumada, S. Shibazaki, M. Takahashi, M. Nagai, Y. Matsuzawa, T. Funahashi, Adiponectin as a biomarker of the metabolic syndrome, Circ. J. 68 (2004) 975–981.

[3] T. Yatagai, S. Nagasaka, A. Taniguchi, M. Fukushima, T. Nakamura, A. Kuroe, Y. Nakai, S. Ishibashi, Hypoadiponectinemia is associated with visceral fat accumulation and insulin resistance in Japanese men with type 2 diabetes mellitus, Metabolism 52 (2003) 1274–1278.

[4] I.P. Lopez, F.I. Milagro, A. Marti, M.J. Moreno-Aliaga, J.A. Martinez, C. De Miguel, High-fat feeding period affects gene expression in rat white adipose tissue, Mol. Cell Biochem. 275 (2005) 109–115.

[5] C. Pitombo, E.P. Araujo, C.T. De Souza, J.C. Pareja, B. Geloneze, L.A. Velloso, Amelioration of diet-induced diabetes mellitus by removal of visceral fat, J. Endocrinol. 191 (2006) 699–706.

[6] J.W. Bullen Jr., S. Bluher, T. Kelesidis, C.S. Mantzoros, Regulation of adiponectin and its receptors in response to development of diet induced obesity in mice, Am. J. Physiol. Endocrinol. Metab. (2006), 15–30.

[7] P.J. Simons, P.S. van den Pangaart, C.P. van Roomen, J.M. Aerts, L. Boon, Cytokine-mediated modulation of leptin and adiponectin secretion during in vitro adipogenesis: evidence that tumor necrosis factor-alpha- and interleukin-1beta-treated human preadipocytes are potent leptin producers, Cytokine 32 (2005) 94–103.

[8] A. Kita, H. Yamasaki, H. Kuwahara, A. Moriuchi, K. Fukushima, M. Kobayashi, T. Fukushima, R. Takahashi, N. Abiru, S. Uotani, E. Kawasaki, K. Eguchi, Identification of the promoter region required for human adiponectin gene transcription: association with CCAAT/enhancer binding protein-beta and tumor necrosis factor-alpha, Biochem. Biophys. Res. Commun. 331 (2005) 484–490.

[9] N. Maeda, M. Takahashi, T. Funahashi, S. Kihara, H. Nishizawa, K. Kishida, H. Nagaretani, M. Matsuda, R. Komuro, N. Ouchi, H. Kuriyama, K. Hotta, T. Nakamura, I. Shimomura, Y. Matsuzawa, PPARgamma ligands increase expression and plasma concentrations of adiponectin, an adipose-derived protein, Diabetes 50 (2001) 2094–2099.

[10] A.D. Kriketos, S.K. Gan, A.M. Poynten, S.M. Furler, D.J. Chisholm, L.V. Campbell, Exercise increases adiponectin levels and insulin sensitivity in humans, Diabetes Care 27 (2004) 629–630.

[11] T. Reinehr, C.L. Roth, U. Alexy, M. Kersting, W. Kiess, W. Andler, Ghrelin levels before and after reduction of overweight due to a low-fat high-carbohydrate diet in obese children and adolescents, Int. J. Obes. (Lond.) 29 (2005) 362–368.

[12] A. Hammarstedt, V.R. Sopasakis, S. Gogg, P.A. Jansson, U. Smith, Improved insulin sensitivity and adipose tissue dysregulation after short-term treatment with pioglitazone in non-diabetic, insulin-resistant subjects, Diabetologia 48 (2005) 96–104.

[13] N. Barth, T. Langmann, J. Scholmerich, G. Schmitz, A. Schaffler, Identification of regulatory elements in the human adipose most abundant gene transcript-1 (apM-1) promoter: role of SP1/SP3 and TNF-alpha as regulatory pathways, Diabetologia 45 (2002) 1425–1433.

[14] J.B. Seo, H.M. Moon, M.J. Noh, Y.S. Lee, H.W. Jeong, E.J. Yoo, W.S. Kim, J. Park, B.S. Youn, J.W. Kim, S.D. Park, J.B. Kim, Adipocyte determination- and differentiation-dependent factor 1/sterol regulatory element-binding protein 1c regulates mouse adiponectin expression, J. Biol. Chem. 279 (2004) 22108–22117.

[15] M. Iwaki, M. Matsuda, N. Maeda, T. Funahashi, Y. Matsuzawa, M. Makishima, I. Shimomura, Induction of adiponectin, a fat-derived antidiabetic and antiatherogenic factor, by nuclear receptors, Diabetes 52 (2003) 1655–1663.

[16] E.J. Henriksen, S. Jacob, T.R. Kinnick, M.K. Teachey, M. Krekler, Selective angiotensin II receptor receptor antagonism reduces insulin resistance in obese Zucker rats, Hypertension 38 (2001) 884–890.

[17] R. Clasen, M. Schupp, A. Foryst-Ludwig, C. Sprang, M. Clemenz, M. Krikov, C. Thone-Reineke, T. Unger, U. Kintscher, PPARgamma-activating angiotensin type-1 receptor blockers induce adiponectin, Hypertension 46 (2005) 137–143.

[18] B. Dahlof, R.B. Devereux, S.E. Kjeldsen, S. Julius, G. Beevers, U. de Faire, F. Fyhrquist, H. Ibsen, K. Kristiansson, O. Lederballe-Pedersen, L.H. Lindholm, M.S. Nieminen, P. Omvik, S. Oparil, H. Wedel, Cardiovascular morbidity and mortality in the Losartan intervention for endpoint reduction in hypertension study (LIFE): a randomised trial against atenolol, Lancet 359 (2002) 995–1003.

[19] S. Julius, S.E. Kjeldsen, M. Weber, H.R. Brunner, S. Ekman, L. Hansson, T. Hua, J. Laragh, G.T. McInnes, L. Mitchell, F. Plat, A. Schork, B. Smith, A. Zanchetti, Outcomes in hypertensive patients at high cardiovascular risk treated with regimens based on valsartan or amlodipine: the VALUE randomised trial, Lancet 363 (2004) 2022–2031.

[20] M. Furuhashi, N. Ura, K. Higashiura, H. Murakami, M. Tanaka, N. Moniwa, D. Yoshida, K. Shimamoto, Blockade of the renin-angiotensin system increases adiponectin concentrations in patients with essential hypertension, Hypertension 42 (2003) 76–81.

[21] R. Negro, G. Formoso, H. Hassan, The effects of irbesartan and telmisartan on metabolic parameters and blood pressure in obese, insulin resistant, hypertensive patients, J. Endocrinol. Invest. 29 (2006) 957–961.

[22] T.W. Kurtz, Treating the metabolic syndrome: telmisartan as a peroxisome proliferator-activated receptor-gamma activator, Acta Diabetol. 42 (2005) S9–S16.

[23] S.C. Benson, H.A. Pershadsingh, C.I. Ho, A. Chittiboyina, P. Desai, M. Pravenec, N. Qi, J. Wang, M.A. Avery, T.W. Kurtz, Identification of telmisartan as a unique angiotensin II receptor antagonist with selective PPARgamma-modulating activity, Hypertension 43 (2004) 993–1002.

[24] M. Takahashi, Y. Arita, K. Yamagata, Y. Matsukawa, K. Okutomi, M. Horie, I. Shimomura, K. Hotta, H. Kuriyama, S. Kihara, T.

Nakamura, S. Yamashita, T. Funahashi, Y. Matsuzawa, Genomic structure and mutations in adipose-specific gene, adiponectin, Int. J. Obes. Relat. Metab. Disord. 24 (2000) 861–868.

[25] H. Mizuguchi, M.A. Kay, A simple method for constructing E1- and E1/E4-deleted recombinant adenoviral vectors, Hum. Gene. Ther. 10 (1999) 2013–2017.

[26] N. Koizumi, H. Mizuguchi, T. Hosono, A. Ishii-Watabe, E. Uchida, N. Utoguchi, Y. Watanabe, T. Hayakawa, Efficient gene transfer by fiber-mutant adenoviral vectors containing RGD peptide, Biochim. Biophys. Acta 1568 (2001) 13–20.

[27] H. Sakaue, W. Ogawa, M. Matsumoto, S. Kuroda, M. Takata, T. Sugimoto, B.M. Spiegelman, M. Kasuga, Posttranscriptional control of adipocyte differentiation through activation of phosphoinositide 3-kinase, J. Biol. Chem. 273 (1998) 28945–28952.

[28] E.D. Rosen, B.M. Spiegelman, Molecular regulation of adipogenesis, Annu. Rev. Cell Dev. Biol. 16 (2000) 145–171, 58:20.

[29] R.J. Perera, E.G. Marcusson, S. Koo, X. Kang, Y. Kim, N. White, N.M. Dean, Identification of novel PPARgamma target genes in primary human adipocytes, Gene. 369 (2006) 90–99, 58:20.

[30] Y. Xu, S.H. Mirmalek-Sani, X. Yang, J. Zhang, R.O. Oreffo, The use of small interfering RNAs to inhibit adipocyte differentiation in human preadipocytes and fetal-femur-derived mesenchymal cells, Exp. Cell Res. 312 (2006) 1856–1864.

[31] Y. Tamori, J. Masugi, N. Nishino, M. Kasuga, Role of peroxisome proliferator-activated receptor-gamma in maintenance of the characteristics of mature 3T3-L1 adipocytes, Diabetes 51 (2002) 2045–2055.

[32] M. Schupp, M. Clemenz, R. Gineste, H. Witt, J. Janke, S. Helleboid, N. Hennuyer, P. Ruiz, T. Unger, B. Staels, U. Kintscher, Molecular characterization of new selective peroxisome proliferator-activated receptor gamma modulators with angiotensin receptor blocking activity, Diabetes 54 (2005) 3442–3452.

[33] T. Yoshida, S. Yamagishi, K. Nakamura, T. Matsui, T. Imaizumi, M. Takeuchi, H. Koga, T. Ueno, M. Sata, Telmisartan inhibits AGE-induced C-reactive protein production through downregulation of the receptor for AGE via peroxisome proliferator-activated receptor-gamma activation, Diabetologia 49 (2006) 3094–3099.

[34] Y. Mori, F. Oana, A. Matsuzawa, S. Akahane, N. Tajima, Short-term effect of bezafibrate on the expression of adiponectin mRNA in the adipose tissues: a study in spontaneously type 2 diabetic rats with visceral obesity, Endocrine 25 (2004) 247–251.

[35] A. Hiuge, A. Tenenbaum, N. Maeda, M. Benderly, M. Kumada, E.Z. Fisman, D. Tanne, Z. Matas, T. Hibuse, K. Fujita, H. Nishizawa, Y. Adler, M. Motro, S. Kihara, I. Shimomura, S. Behar, T. Funahashi, Effects of Peroxisome Proliferator-Activated Receptor Ligands, Bezafibrate and Fenofibrate, on Adiponectin Level, Arterioscler. Thromb. Vasc. Biol. (2006), 58:20.

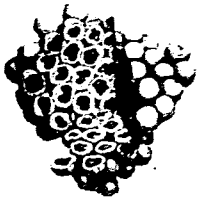

STEM CELLS®

Targeted Delivery of CX3CL1 to Multiple Lung Tumors by Mesenchymal Stem Cells

Hong Xin, Masahiko Kanehira, Hiroyuki Mizuguchi, Takao Hayakawa, Toshiaki Kikuchi, Toshihiro Nukiwa and Yasuo Saijo

Stem Cells 2007;25;1618-1626; originally published online Apr 5, 2007;
DOI: 10.1634/stemcells.2006-0461

STEM CELLS

TRANSLATIONAL AND CLINICAL RESEARCH: MESENCHYMAL STEM CELLS SERIES

Targeted Delivery of CX3CL1 to Multiple Lung Tumors by Mesenchymal Stem Cells

HONG XIN,[a] MASAHIKO KANEHIRA,[a,b] HIROYUKI MIZUGUCHI,[c] TAKAO HAYAKAWA,[d] TOSHIAKI KIKUCHI,[b] TOSHIHIRO NUKIWA,[b] YASUO SAIJO[a]

[a]Department of Molecular Medicine, Tohoku University Graduate School of Medicine, Sendai, Japan; [b]Department of Respiratory Oncology and Molecular Medicine, Institute of Development, Aging, and Cancer, Tohoku University, Sendai, Japan; [c]Laboratory of Gene Transfer and Regulation, National Institute of Biomedical Innovation, Osaka, Japan; [d]Pharmaceutical and Medical Devices Agency, Tokyo, Japan

Key Words. Mesenchymal stem cell • Gene therapy • Multiple tumors • Lung metastases

ABSTRACT

MSCs are nonhematopoietic stem cells capable of differentiating into various mesoderm-type cells. MSCs have been considered to be a potential vehicle for cell-based gene therapy because MSCs are relatively easily expanded in vitro and have the propensity to migrate to and proliferate in the tumor tissue after systemic administration. Here, we demonstrated the tropism of mouse MSCs to tumor cells in vitro and multiple tumor tissues in the lung after i.v. injection of green fluorescent protein-positive MSCs in vivo. We transduced CX3CL1 (fractalkine), an immunostimulatory chemokine, to the mouse MSCs ex vivo using an adenoviral vector with the Arg-Gly-Asp-4C peptide in the fiber knob. Intravenous injection of CX3CL1-expressing MSCs to the mice bearing lung metastases of C26 and B16F10 cells strongly inhibited the development of lung metastases and thus prolonged the survival of these tumor-bearing mice. This antitumor effect depended on both innate and adaptive immunity. These results suggest that MSCs can be used as a vehicle for introducing biological agents into multiple lung tumor tissues. STEM CELLS *2007;25:1618–1626*

Disclosure of potential conflicts of interest is found at the end of this article.

INTRODUCTION

The high doses of biological agents needed to obtain clinical effects in cancer therapy often cause excessive toxicity. Gene therapies expressing these biological agents have been considered because the biological agents can be introduced exclusively into the tumor milieu rather than the systemic circulation. An optimal gene delivery vector should show efficient targeting to multiple tumor tissues, efficient gene transduction to the tumor cells, and high expression of transgenes in the tumors. However, to date, no vectors meeting all these requirements have been developed.

Some types of cells migrate to and reside in the tissues after systemic injection. Therefore, genetically modified cells coupling cell therapy and gene therapy may be able to deliver certain genes to the target sites. Several types of cells, including fibroblasts [1], endothelial cells [2], dendritic cells [3], and tumor-infiltrating lymphocytes [4–6], have been used to deliver therapeutic agents into tumor tissues. However, difficulties related to in vitro cell expansion, low efficiency of gene transfer to the cells, or the need for direct injection to the tumor tissue because of poor migration to the tumor sites have limited the clinical application.

Bone marrow-derived MSCs are adherent, nonhematopoietic cells that reside within the bone marrow stroma and regulate the differentiation of hematopoietic stem cells [7]. These cells are pluripotent and have the ability to differentiate into various mesoderm-type cells, osteoblasts, adipocytes, chondrocytes, myoblasts, and endothelial precursor cells [8–10]. Because MSCs can be relatively easily expanded in vitro and retain an extensive multipotent capacity for differentiation, they are being used to develop therapies for tissue regeneration in animal models [9–11]. Recent data revealed another important biological feature of MSCs. MSCs can selectively migrate to and proliferate in solid tumors after systemic injection and become stromal cells [12]. A few studies have reported that systemic administration of genetically modified MSCs targeting to multiple tumor sites showed antitumor effects in animal tumor models [13–15].

Although adenoviral vectors efficiently infect and highly express the transgene in many types of cells, high titers of the adenoviral vector would be needed to increase the efficiency of transduction into MSCs because of the poor expression of coxsackie adenovirus receptor (CAR) in MSCs [16]. It has previously been shown that an adenoviral vector with the Arg-Gly-Asp (RGD)-4C peptide in the fiber knob (AdRGD) increased the tropism and thus improved the efficacy of transduction into MSCs by over 10 times [16, 17].

CX3CL1 fractalkine is a member of CX3CL and exists in both a membrane-bound form and a soluble form. The soluble form of CX3CL1 induces the migration of cell expressing its receptor, CX3CR1, in a manner similar to that of other soluble chemokines [18–20]. We have previously demonstrated that intratumoral injection of an adenoviral vector expressing CX3CL1 induced strong antitumor effects through the activa-

Correspondence: Yasuo Saijo, M.D., Ph.D., Department of Molecular Medicine, Tohoku University Graduate School of Medicine, 2-1 Seiryomachi Aobaku, Sendai 980-8575, Japan. Telephone: 81-22-717-8230; Fax: 81-22-717-7882; e-mail: yasosj@idac.tohoku.ac.jp
Received July 23, 2006; accepted for publication March 28, 2007; first published online in STEM CELLS *EXPRESS* April 5, 2007 ©AlphaMed Press 1066-5099/2007/$30.00/0 doi: 10.1634/stemcells.2006-0461

tion of both natural killer (NK) cells and T cells [21]. This treatment affected only the tumors injected with the adenoviral vector but not distant tumors. Therefore, our goal was to develop an effective gene therapy for multiple tumors by MSCs.

In this study, we infected MSCs with AdRGD expressing CX3CL1 and administered them systemically to tumor-bearing mice. Systemic administration of MSCs expressing CX3CL1 resulted in a strong inhibitory effect on lung metastases and thus prolonged the survival of the tumor-bearing mice.

MATERIALS AND METHODS

Cell Culture and Mice

The murine colon adenocarcinoma cell line C26 (H-2^d), melanoma cell line B16F10 (H-2^b), and fibroblast cell line BLKCL4 (H-2^b) were obtained from the Cell Resource Center for Biomedical Research (Tohoku University, Sendai, Japan). These cell lines were grown in RPMI 1640 medium with 10% fetal bovine serum (FBS). The murine fibroblast cell line BALB 3T3 cells (H-2^d) were purchased from the Health Science Research Resources Bank (National Institute of Biomedical Innovation, Osaka, Japan) and were propagated in Dulbecco's modified Eagle's medium with 10% FBS. The cell viability was assayed by a cell viability assay kit (Alamar Blue; Biosource International, Camarillo, CA, http://www.biosource.com) according to the manufacturer's instructions. Female C57BL/6 (H-2^b) mice, BALB/c (H-2^d) mice, and BALB/C nude mice, 6–8 weeks old, were purchased from Charles River Laboratories Japan (Atsugi, Japan, http://www.criver.com). Green fluorescent protein (GFP)-expressing mice (C57BL/6-TgN [ACTbEGFP]) were kindly provided by Dr. M. Okabe (Osaka University, Osaka, Japan). $CD8^+$ T-cell-deficient (B6.129S2-Cd8α^{tm1Mak}) mice that had been backcrossed to the C57BL/6 background were obtained from Jackson Laboratory (Bar Harbor, ME, http://www.jax.org). All animal experiments were approved by the institutional review board for animal experiments of Tohoku University.

Isolation and Culture of Mouse MSCs

The bone marrow of 6–10-week-old BALB/c, C57BL/6, or GFP-expressing mice was flushed out with cultured medium and expelled from a 5-ml syringe through a 25-gauge needle. The marrow suspension was then transferred to six-well plates at a concentration of 1.5×10^6 nucleated cells per cm^2. The cells were cultured in low glucose Dulbecco's modified Eagle's medium (DMEM) (Gibco-BRL, Grand Island, NY, http://www.gibcobrl.com) with 10% FBS (Gibco-BRL). After 72 hours, nonadherent cells were removed, and fresh medium was added. When the adherent cells reach 70%–80% confluence, the cells were trypsinized (0.05% trypsin for 3 minutes), harvested, and expanded. When a homogenous cell population was obtained after 3–5 passages, these cells were used for the subsequent experiments.

The induction of adipogenic differentiation from MSCs was performed according to the report by Arai et al. [22]. MSCs were cultured with 0.5 mM 3-isobutyl-1-methylxanthine (Sigma-Aldrich, St. Louis, http://www.sigmaaldrich.com), 1 μM dexamethasone (Dex), 10 mg/ml insulin, and 10% FBS in DMEM (adipogenic induction medium) for 1 week. Then, the medium was changed to adipogenic maintenance medium (10% FBS in DMEM containing 1 μM Dex and 10 mg/ml insulin) and cultured for an additional 4 days. The cells were fixed in 10% formalin for 10 minutes and stained for 20 minutes with fresh oil red O (Sigma-Aldrich) solution. Osteogenic differentiation was induced by culturing cells for 3 weeks in DMEM supplemented with 10% FBS, 0.2 μM ascorbic acid (Sigma-Aldrich), 10 mM β-glycerophosphate (Sigma-Aldrich), and 0.1 μM dexamethasone (Sigma-Aldrich). The medium was changed every 3 days. Osteogenic differentiation was detected by Alizarin red S (Sigma-Aldrich) staining.

Adenoviral Vectors

A replication-deficient recombinant adenoviral vector carrying the *β-galactosidase reporter* gene LacZ (AdLacZ) under the control of the cytomegalovirus promoter was constructed as previously reported [21]. A genetically modified adenoviral vector with an integrin-binding motif (Arg-Gly-Asp) in the HI loop of the fiber knob carrying fractalkine and β-galactosidase (AdRGDFKN and AdRGDLacZ) was also constructed as previously reported [23, 24]. These recombinant adenoviral vectors were propagated using 293 cells and purified by CsCl gradient centrifugation. The total numbers of viral particles in the viral sample were measured by optical density (OD_{260}) (where an OD_{260} of 1 is equal to 10^{12} particles). The titers (expressed as plaque-forming units [pfu] per milliliter) of the viral stocks were quantified by a plaque-forming assay using 293 cells.

β-Galactosidase Staining

To determine the expression of β-galactosidase after AdLacZ or AdRGDLacZ vector infection, the MSCs were plated 24 hours before infection and incubated with the adenoviruses at different multiplicities of infection (MOIs) for 48 hours. LacZ expression by adenoviral vector (Ad)-transduced MSCs was evaluated by staining with a β-galactosidase (β-gal) staining kit (Invitrogen, Carlsbad, CA, http://www.invitrogen.com).

Expression of CX3CL1 Fractalkine and Its Receptor CX3CR1 on MSCs

To determine the fractalkine expression after AdRGDFKN infection (100 MOI), the total cellular RNA was extracted from the AdRGDFKN-transduced (or control-transduced) MSCs (MSCs/RGDFKN) using Isogen (Nippon Gene, Tokyo, http://www.nippongene.com) after 24 hours of infection. Total RNA (2 μg) was converted into cDNA by oligo$(dT)_{12-18}$ primers and Superscript II reverse transcription (Gibco-BRL) in a final volume of 20 μl. One microliter of this cDNA was amplified with the following primers specific for either vector-derived fractalkine (FKN) or the control β-actin transcripts: for endogenous FKN, 5′-GTCAGCACCTCGGCATGACGAAATG-3 (sense); for exogenous FKN, 5′-TGCCAAGAGTGACGTGTCCA-3 (sense) and 5′-CACTGGCACCAGGACGTATG-3′ (antisense); for CX3CR1, 5′-TTCGGTCTGG TGGGAAATCTG-3 (sense) and 5′-CGTCTGGATGCGGAAGTAG-3 (antisense); for β-actin, 5′-CTCTTTGATGTCACGCACGATTTC-3′ and 5′-GTGGGCCGCTCTAGGCACCAA-3′. The amplification profile was 95°C for 5 minutes and 30 cycles of 95°C for 30 seconds, 55°C for 30 seconds, and 72°C for 60 seconds.

To assess the fractalkine expression on the cell membrane of MSCs, after 48-hour infection of AdRGDFKN, the cells were washed twice with phosphate-buffered saline (PBS), fixed in 4% paraformaldehyde for 10 minutes, and stained for 30 minutes with a rat monoclonal antibody to murine fractalkine (20 μg/ml) or nonspecific control rat IgG antibodies followed by fluorescein isothiocyanate (FITC)-conjugated secondary antibody. Cells were then visualized after 4,6-diamidino-2-phenylindole counterstaining and examined by fluorescent microscopy. The secreted form of fractalkine in the supernatant of MSCs was measured by enzyme-linked immunosorbent assay (ELISA) (R&D Systems Inc., Minneapolis, http://www.rndsystems.com) according to the manufacturer's instructions. The assay was performed in triplicate.

In Vitro and In Vivo Migration Assay

To examine the biological activity of CX3CL1 secreted from MSCs/RGDFKN, a cell migration assay was carried out as described previously [21]. THP-1 cells (5×10^5 in 100 μl) were seeded in the upper wells of a transwell plate (24-well plate) with a polycarbonate membrane having a 5-μm pore size (Corning Costar, Corning, NY, http://www.corning.com/lifesciences). The lower wells were filled with 600 μl of medium containing supernatants of MSCs/RGDFKN at different doses of MOIs for 48 hours. After a 3-hour incubation at 37°C, the number of cells that migrated through the polycarbonate membrane were harvested from the lower chamber and counted under a microscope. The assay was performed in triplicate. The tropism of MSCs for tumor cells was

determined using an in vitro migration assay according to previously described methods [15]. MSCs or fibroblasts (BLKCL4) were suspended at 3×10^6 cells per milliliter in 0.5% FBS containing DMEM, and 100 μl of these cell suspensions were loaded into the upper well of transwell plates (8-μm pore membranes; Corning Costar Inc.). Cell-free medium conditioned by B16F10 cells for 48 hours with 0.5% FBS was put in the lower wells. The MSCs or fibroblasts were allowed to migrate across the membrane for 3 hours at 37°C. After 3 hours, the membrane was disassembled from the chambers, and the cells that remained attached to both sides of the membrane were fixed with methanol. After staining of the cells using a Diff-Quick staining kit (International Reagents Corp., Kobe, Japan), the cells attached to the upper side of the membrane were wiped away, and the cells that migrated to the lower side of the membrane were counted. Cell numbers were expressed as the average number of migrated cells in 10 random fields. The assays were performed in triplicate.

To examine the ability of MSCs to migrate toward tumor tissues in vivo, 7 days after i.v. injection of MSCs or fibroblasts of GFP mice (5×10^5 cells per mouse) into mice with or without established B16F10 pulmonary metastases, halves of organs (lung, liver, kidney, spleen, and bone marrow) were fixed with 4% paraformaldehyde and embedded in paraffin. Halves were used for fluorescence-activated cell sorting (FACS). Sections were treated by autoclave-based antigen-retrieval technique with 10 mM citrate buffer at pH 6.0 and 120°C for 10 minutes. After blocking nonspecific staining and endogenous peroxidase, sections were incubated for 1 hour with rabbit polyclonal anti-GFP antibody (Molecular Probes Inc., Eugene, OR, http://probes.invitrogen.com) and then with Simple Stain Mouse MAX PO (Nichirei, Tokyo, http://www.nichirei.co.jp/english) for 60 minutes and applied to AEC reagents (Nichirei). The specimens were then incubated with hematoxylin for nuclear counterstaining.

Measurement of CX3CL1 Concentration in Lung Tissues

Seven days after MSCs/RGDFKN injection into mice with lung metastases, mice were sacrificed, and the pulmonary circulation was perfused with saline via the right ventricle. The whole lung was homogenized in 1 ml of homogenizing buffer (Hanks' balanced salt solution, pH 7.1) using a tissue homogenizer. The lung homogenates were centrifuged at 15,000 rpm for 20 minutes to sediment tissue debris, and the supernatants were subjected to the ELISA (R&D Systems, Minneapolis, MN, http://www.rndsystems.com) to the measure the fractalkine concentration.

Treatment of Lung Metastases by AdRGDFKN-Transduced MSCs

To establish experimental lung metastases, 5×10^5 tumor cells in 0.2 ml of PBS were injected into the lateral tail vein of the mice (B16F10 into C57BL/6, C26 into BALB/c) (day 0). Five days later, the mice were randomly divided into five groups. Sixteen mice were allocated to each group in all experiments. Mice in the first group received an i.v. injection of 5×10^5 MSCs/RGDFKN. Mice in the second group received an i.v. injection of 5×10^5 MSCs/RGDLacZ as a control for AdRGDFKN. Mice in the third group received an i.v injection of 5×10^5 fibroblasts/RGDFKN as a control for MSCs. Mice in the fourth group received an i.v. injection of AdRGDFKN vector (5×10^7 pfu) without any cells. Mice in the fifth group received an i.v. injection of PBS alone. Eight mice of each group were sacrificed at day 12, and the lungs were fixed in Bouin's solution. The metastatic colonies were easily identified macroscopically by demarcated black or white nodules on the lung surface. The numbers of metastatic nodules on the lung surface were counted three times per sample. The other eight mice of each group were monitored until death for the survival assay. Survival curves were drawn by the Kaplan-Meier method.

Histological Analyses of Infiltrating Immune Cells into Tumors

Three days after i.v. injection of MSCs/RGDFKN, frozen sections of the lung were incubated with optimal dilutions of the primary antibodies, including anti-mouse CD4 (RM4–5; BD Pharmingen, San Diego, http://www.bdbiosciences.com/pharmingen), CD8 (KT15; Serotec Ltd., Oxford, U.K., http://www.serotec.com), rabbit anti-asialo GM1 (Wako Chemical, Osaka, Japan, http://www.wako-chem.co.jp/english), or isotype matched IgG for 30 minutes. For CD4 and CD8, the sections were then incubated with biotin-labeled second antibody for 30 minutes, followed by streptavidin-horseradish peroxidase. For NK, the sections were incubated with Simple Stain Mouse MAX PO (Nichirei) and then applied to Simple Stain AEC reagents (Nichirei). The specimens were then incubated with hematoxylin for nuclear counterstaining.

For flow cytometry, lung tissues were minced and then incubated for 90 minutes at 37°C in 3% FBS containing medium (3 ml per lung) supplemented with collagenase I (0.7 mg/ml; Roche Diagnostics, Mannheim, Germany, http://www.roche-applied-science.com) and DNase I (30 μg/ml; Roche Diagnostics). After incubation, a single-cell suspension was collected by removing large aggregates and debris by passage through a 70-μm Falcon cell strainer (Becton, Dickinson and Company, Franklin Lakes, NJ, http://www.bd.com) and resuspended at 5×10^6 cells per milliliter for antibody staining (FITC-conjugated monoclonal rat anti-mouse IgGs against CD4, CD8, and NK1.1, respectively [BD Pharmingen]). The cells were then exposed to propidium iodide (1 μg/ml in PBS) to identify dead cells. These cells were analyzed on an EPICS XL cytometer with EXPO32 ADC software (Beckman Coulter, Miami, FL, http://www.beckmancoulter.com). Each group had more than three mice.

Treatment of Lung Metastases in $CD8^{-/-}$ and NK-Depleted Mice

$CD8^{-/-}$ mice received an i.v. injection of 5×10^5 MSCs/RGDFKN or PBS 5 days after the injection of 5×10^5 B16F10 cells into the lateral tail vein. For NK cell depletion, C57BL/6 mice were treated with asialo GM1 antiserum (200 μg per mouse) (Wako Chemical) or the same dose of control IgG by intraperitoneal injection five times on days −3, −2, −1, 4, and 9. Using anti-NK1.1 antibody, it was determined that the $NK1.1^+$ population was less than 1% [21]. These NK-depleted mice and control IgG-injected mice were transplanted with B16F10 on day 0 and treated with an i.v. injection of 5×10^5 MSCs/RGDFKN or PBS on day 5. Each group had eight mice.

Statistical Analysis

The results were expressed as mean ± SE or as mean ± SD. Statistical comparisons were made using the two-tailed Student's t test, and a value of $p < .05$ was accepted as indicating significance. For the survival data, the log-rank test was used to assess differences among the five treatment groups, and a p value of less than .05 was considered statistically significant.

RESULTS

Differentiation of MSCs and Improvement of Transduction Efficiency by RGD Fiber-Modified Ad Vector

MSCs cultured at passage 5 readily differentiated into adipocytes when incubated in adipogenic maintenance medium and differentiated into osteoblasts following supplementation of the medium with osteogenic induction medium (data not shown). The MSCs used in this study retained their differentiation capability. MSCs transduced with AdRGDFKN also could differentiate to adipocytes and osteoblasts (data not shown). 5-Bromo-4-chloro-3-indolyl-β-D-galactopyranoside staining revealed that more than 80% of MSCs infected with 200 MOI of AdRGDLacZ were positive for β-galactosidase, whereas AdLacZ-infected MSCs were scarcely stained (< 5%) (Fig. 1B, 1C). These results demonstrated that the gene delivery and the expression of transgenes in the MSCs by the $\alpha v\beta$ integrin-target-

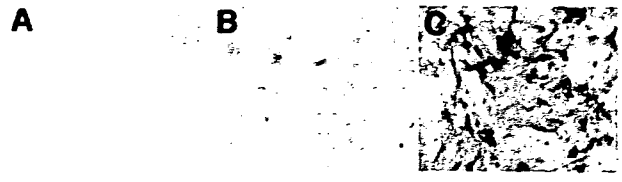

Figure 1. LacZ expression in mouse MSCs infected with adenoviral vector carrying β-galactosidase (AdRGDLacZ) (**A–C**). Shown are photomicrographs of MSCs stained with β-galactosidase. MSCs were transduced with phosphate-buffered saline (**A**), adenoviral vector carrying the *β-galactosidase reporter* gene LacZ (AdLacZ) (**B**), or AdRGDLacZ (**C**).

ing adenoviral vector were more efficient than those by using conventional unmodified adenoviral vectors.

CX3CL1 Expression in MSCs/RGDFKN and Its Function

The expression of CX3CL1 FKN by MSCs/RGDFKN in vitro was confirmed by reverse transcription-polymerase chain reaction and confocal microscopy (Fig. 2). In contrast to the low level of endogenous FKN mRNA expression in control MSCs, a high level of FKN mRNA expression was detected only in MSCs/RGDFKN. Exogenous transcripts of fractalkine were detected only in MSCs/RGDFKN (Fig. 2A). Similar levels of endogenous CX3CR1 mRNA expression were detected in all MSCs (data not shown). MSCs/RGDFKN expressed fractalkine on the cellular membrane and cytoplasm, but control MSCs and MSCs/RGDLacZ had no fractalkine expression by confocal microscopic analyses (Fig. 2B). The CX3CL1 concentration of the supernatants from MSCs/RGDFKN increased in a manner that was dose-dependent on the MOIs and reached a peak and plateau at 70 MOI (Fig. 2C). The biological activity of secreted fractalkine from MSCs/RGDFKN was determined by cell migration assay using THP-1 cells (Fig. 2D). The supernatants of MSCs/RGDFKN mediated chemotaxis of THP-1 cells. These results indicated that MSCs/RGDFKN secrete biologically active soluble CX3CL1.

Tropism of MSCs for Tumors In Vitro and In Vivo

Since recent studies reported that MSCs migrate to tumors and contribute to the formation of stromal tissues [12], we performed in vitro migration assays using transwell plates as a surrogate assay for the tropism of MSCs. The medium conditioned by B16F10 cells induced a significant increase of MSC migration by 2.5-fold ($p < .001$) compared with the cell-free medium, whereas it did not increase the number of migrating cells of BLKCL4 fibroblasts (Fig. 3A). Fibroblasts were chosen as control cells because MSCs were originally described as fibroblastic colony-forming cells and because fibroblasts are morphologically similar to MSCs.

To evaluate the migration of MSCs into the tumor tissues of the lung, GFP-positive MSCs or fibroblasts were injected into the lateral tail vein of C57BL/6 mice carrying B16F10 lung metastases. GFP-positive MSCs were found mostly within and surrounding tumor tissues (Fig. 3Ba), but there were few such cells in the normal lung (Fig. 3Bd). However, GFP-positive fibroblasts were not found either in the tumor tissues or normal lung (Fig. 3Bb, 3Be). No GFP-positive cells were detected in areas of the lung injected only with PBS (Fig. 3Bc, 3Bf). In the non-tumor-bearing nude mice, we found very few GFP-positive MSCs (less than three cells in one slide) in the lung, liver, spleen, and bone marrow, but not heart muscle, 7 days after MSC injection. The results suggested that the MSCs have specific migratory activity toward tumor tissues in vivo.

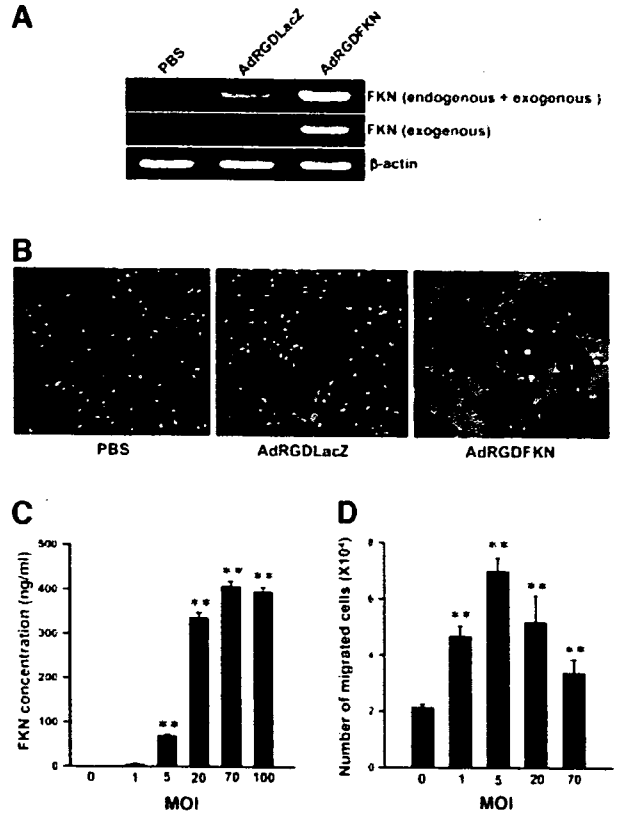

Figure 2. CX3CL1 fractalkine expression on MSCs/RGDFKN. (**A**): Detection of fractalkine transcript expression by reverse transcription-polymerase chain reaction in MSCs transduced with AdRGDFKN or AdRGDLacZ. (**B**): A representative microphotograph of MSCs stained with anti-mouse fractalkine monoclonal antibody (magnification, ×200). (**C**): Enzyme-linked immunosorbent assay of supernatants of MSCs/RGDFKN at different MOIs. Each value represents the mean ± SD ($n = 3$). (**D**): Chemotaxis of THP-1 cells in response to culture supernatants of MSCs/RGDFKN (MOI as indicated). Each value represents the mean ± SD of number of migration cells counted in eight high-power fields from three experiments; **, $p < .01$. Abbreviations: AdRGDFKN, adenoviral vector carrying fractalkine; AdRGDLacZ, adenoviral vector carrying β-galactosidase; FKN, fractalkine; MOI, multiplicity of infection; PBS, phosphate-buffered saline.

As the next step, we determined whether MSCs/RGDFKN expressed CX3CL1 in the lung tumor tissues by ELISA. Treatment of MSCs/RGDFKN increased the CX3CL1 contents in the lung with metastases, but not in the normal lung (Fig. 3C).

Effects of Systemic Administration of MSCs/RGDFKN on the C26 Lung Metastases

We next examined the in vivo effects of MSCs/RGDFKN in the C26 lung metastasis model. MSCs/RGDFKN (5×10^5) were injected intravenously once on day 5 after the injection of C26 cells. Control mice received PBS, MSCs/RGDLacZ as a control for AdRGDFKN, BALB 3T3/RGDFKN as a control for MSCs, or 5×10^7 pfu AdRGDFKN, a dose equivalent to that for infection of MSCs ex vivo. The mice treated with MSCs/RGDFKN developed fewer and smaller metastatic nodules on the lung surface than the mice of the other treatment groups (Fig. 4A). Microscopic observation of the lung confirmed that only mice treated with MSC/RGDFKN developed fewer and smaller nodules than the other treatment groups (Fig. 4B). When the metastatic nodules on the lung surface were counted macroscopically, treatment with MSCs/RGDFKN was shown to

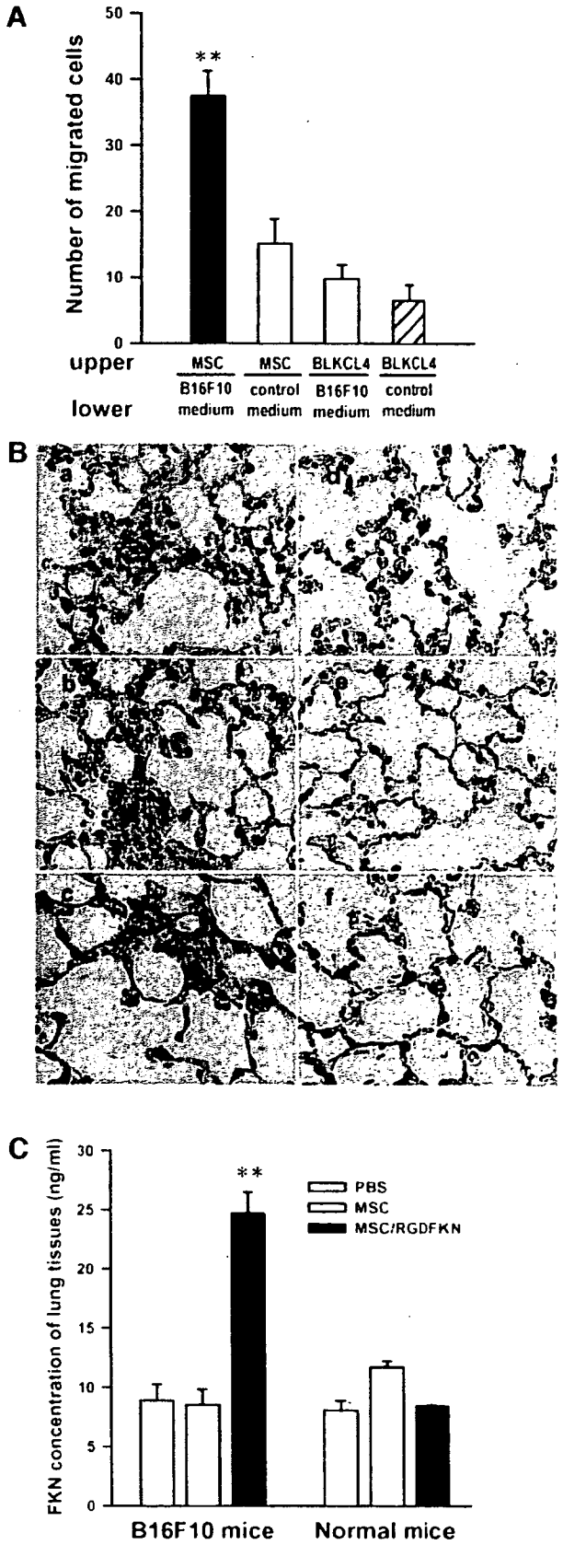

have significantly reduced the number of lung metastases compared with any other controls ($p < .01$). Although mice treated with AdRGDFKN alone showed reduced numbers of metastatic nodules, the inhibitory effect was minimal (36%) compared with PBS and was not statistically significant ($p = .83$). Mice treated with either MSCs/RGDLacZ or BALB 3T3/RGDFKN did not demonstrate any reduction of lung metastases (Fig. 4C).

The mice treated with MSCs/RGDFKN lived significantly longer than the mice of any other treatment groups ($p < .001$) (Fig. 4D). The median survival time of the mice treated with MSCs/RGDFKN was the longest (30 days) among the treatment groups (17–20 days). Although the mice treated with 5×10^7 pfu AdRGDFKN lived significantly longer than the mice treated with PBS or BALB 3T3/RGDFKN ($p < .005$), the prolongation of the survival time was less than that in MSCs/RGDFKN (Fig. 4D).

Effects of Systemic Administration of MSCs/RGDFKN on the B16F10 Lung Metastases

We also examined the in vivo effects of MSCs/RGDFKN in the B16F10 lung metastasis model. Again, mice treated with MSCs/RGDFKN developed fewer and smaller metastatic nodules on the lung surface than the mice of the other treatment groups (Fig. 5A, 5B). The number of metastatic nodules in mice treated with MSCs/RGDFKN was markedly reduced by 84% compared with the PBS control ($p < .005$) (Fig. 5C). Although treatment with MSCs/RGDLacZ reduced metastatic nodules by 43%, this reduction was not statistically significant ($p = .3$). The mice treated with either 5×10^7 pfu AdRGDFKN or BLKCL4/RGDFKN did not demonstrate any reduction in lung metastases (Fig. 5C).

In the survival analysis, the mice treated with MSCs/RGDFKN lived significantly longer than the mice of the other groups ($p < .05$) (Fig. 5D). The prolongation of survival in the B16F10 model by MSCs/RGDFKN was shorter than in the C26 model. The mice injected with B16F10 cells developed metastases not only in lung but also in other organs, including the liver, kidney, ovary, nerve roots of the cauda equina, skin, and so on. The mice treated with MSCs/RGDFKN died mainly of metastases of the skin and nerve roots of the cauda equina.

NK Cells and $CD8^+$ T Cells Were Involved in the MSCs/RGDFKN-Mediated Antitumor Effects

To investigate the mechanisms of the antitumor effects by MSCs/RGDFKN, histological analyses in the tumors were performed on day 3 after MSCs/RGDFKN treatment. Metastatic lung tumors treated by MSCs/RGDFKN showed infiltrations of $CD8^+$ lymphocytes, CD4 lymphocytes, and NK cells compared

Figure 3. Tropism of MSCs for tumor cells in vitro and in vivo and CX3CL1 concentration of the lung tissues. **(A):** Migration of MSCs in response to the medium conditioned by B16F10 cells. The numbers of MSCs that migrated to the lower chamber were counted after 3 hours incubation. BLKCL4 fibroblasts were used as a control for MSCs. Each value represents the mean ± SD of number of migrating cells counted in 10 fields from three experiments; **, $p < .01$. **(B):** Detection of GFP-positive cells after i.v. injection of MSCs or fibroblasts derived from GFP-transgenic mice. The lungs with or without metastases of B16F10 were removed 7 days after i.v. injection of MSCs or fibroblasts. Left panels, lung tissues with metastases. Right panels, lung tissues without metastases. **(Ba, Bd):** Lungs after MSC injection. **(Bb, Be):** Lungs after fibroblast injection. **(Bc, Bf):** Lungs after PBS injection (magnification, ×400). **(C):** Mice with established B16F10 tumors in the lung were injected intravenously with MSCs/RGDFKN (5×10^5). The mice were sacrificed after 3 days, and lung homogenates were subjected to the enzyme-linked immunosorbent assay for CX3CL1. Each group had five mice; **, $p < .01$. Abbreviations: FKN, fractalkine; PBS, phosphate-buffered saline; RGDFKN, AdRGD expressing fractalkine.

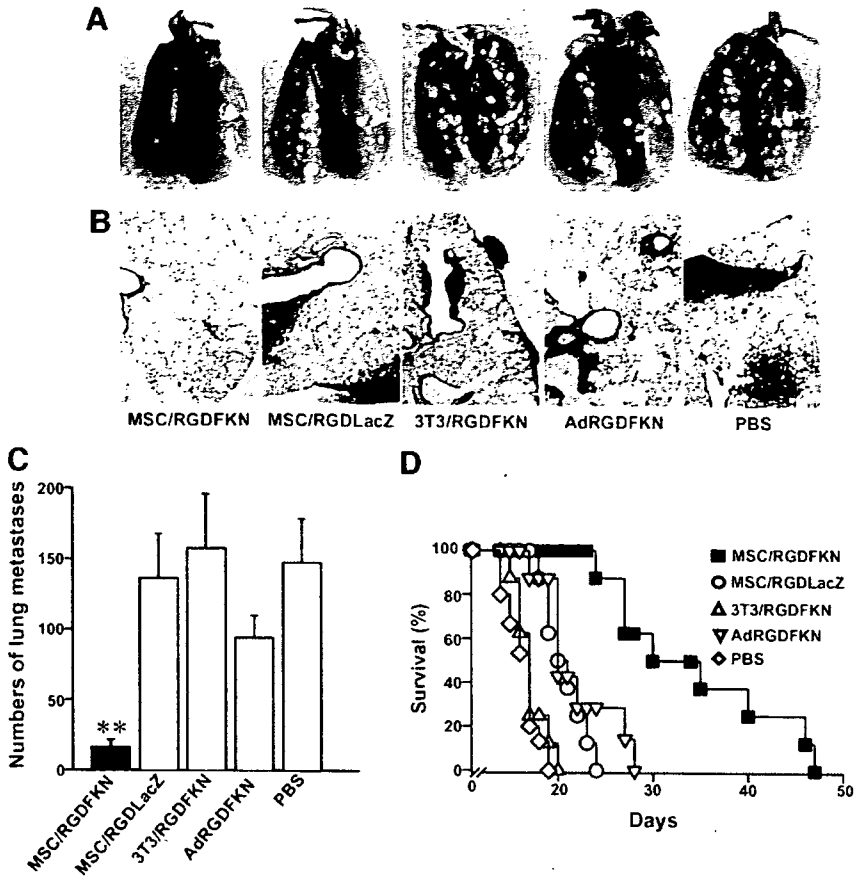

Figure 4. Inhibition of C26 lung metastases by i.v. injection of MSCs/RGDFKN. C26 cells (5×10^5) were injected into the lateral tail vein of BALB/c mice (day 0). Five days later, mice were treated with i.v. injection of MSCs/RGDFKN (5×10^5 cells) or MSCs/RGDLacZ, i.v. injection of 3T3/RGDFKN, i.v. injection of AdRGDFKN vector (5×10^7 plaque-forming units), or PBS alone. **(A):** A representative macrograph of C26 pulmonary metastases on the lung surface in each treatment group. **(B):** A representative micrograph of C26 pulmonary metastases stained with H&E in each treatment group. **(C):** Numbers of pulmonary metastatic nodules in each treatment group. The numbers of metastatic nodules on the lung surface were counted macroscopically. The data represent the mean ± SD of results from eight mice. **, $p < .01$. **(D):** Mice with established pulmonary metastases of C26 were treated as described above. ■, MSCs/RGDFKN; ○, MSCs/RGDLacZ; △, 3T3/RGDFKN; ▽, AdRGDFKN vector; ◇, PBS. Survival curves were drawn by the Kaplan-Meier method ($n = 8$ in each treatment group). Abbreviations: AdRGDFKN, adenoviral vector carrying fractalkine; PBS, phosphate-buffered saline; RGDFKN, AdRGD expressing fractalkine; RGDLacZ, AdRGD expressing *β-galactosidase reporter* gene LacZ.

with controls (Fig. 6A). Quantification of these leukocytes by FACS revealed significant infiltration of $CD8^+$ lymphocytes and NK cells ($p < .05$) (Fig. 6B), whereas no statistically significant increase of $CD4^+$ T lymphocytes was observed.

To functionally delineate the role of $CD8^+$ T cells and NK cells, we used NK-depleted mice and $CD8^{-/-}$ mice. Treatment by MSCs/RGDFKN did not show any inhibitory effect on B10F10 lung metastases in NK-depleted mice (Fig. 7A), whereas IgG-treated control mice responded to the treatment of MSCs/RGDFKN. In the $CD8^{-/-}$ mice, treatment by MSCs/RGDFKN again did not show any inhibitory effect (Fig. 7B). These results confirmed our previously reported finding that the antitumor effects by fractalkine depend on both NK and $CD8^+$ T cells [21].

Discussion

In this study, we demonstrated that i.v. injection of mouse MSCs expressing CX3CL1 migrated to the tumor tissues of the lung and secreted CX3CL1 to the tumor milieu. MSCs/RGDFKN induced both innate and adaptive immunity, thus inhibiting multiple lung metastases and prolonging survival. We also confirmed the higher transduction efficacy of the AdRGD vector into MSCs compared with that of the Ad5-based regular adenoviral vector.

In our study, MSCs but not fibroblasts migrated to the culture supernatant of B16F10 cells in vitro. MSCs injected intravenously migrated to the tumor tissues of the lung, but there were only a few in other, normal tissues, as we demonstrated using GFP-positive MSCs, as reported previously [14]. However, we could not demonstrate colony formation of MSCs in the tumor tissues. No colony formation of MSCs might be attributed to the difficulty of expanding mouse MSCs or the short period after MSC injection. The concentration of CX3CL1 in the lung with metastases was significantly increased compared with controls. In addition, the fact that systemic administration of fibroblasts expressing CX3CL1 did not show any inhibitory effects on lung metastasis in C26 or B16F10 suggests that MSCs indeed stayed in the tumor tissues rather than just passing into the vascular circulation of the lung.

Hung et al. recently provided direct evidence for microscopic tumor targeting by exogenously administered human MSCs [12]. They used positron emission tomography (PET) imaging with [18F]-9-(4-fluoro-3-hydroxymethylbutyl)-guanine to monitor the genetically modified herpes simplex virus type 1 thymidine kinase and enhanced green fluorescent protein expressing human MSCs. In vivo PET imaging revealed that human MSCs could target microscopic tumors, proliferate, differentiate, and contribute to the formation of tumor stroma. Although the precise molecular mechanisms by which MSCs migrate to tumor tissues are still unknown, the mechanisms of migration of MSCs to injured organs are beginning to be understood. A subpopulation of MSCs expresses a restricted set of chemokine receptors and shows chemotactic migration in response to the chemokine in vitro [25]. In an in vivo model, this chemotactic migration was principally mediated by CX3CL1 and CXCL12 [26]. Since injured or inflammatory tissues upregulate CXCL12 and CX3CL1, the migration of MSCs to the injured tissues is regulated by the interaction between CXCR4/CXCL12 and CX3CR1/CX3CL1. Moreover, a recent study demonstrated that MSCs express functional c-met and exhibit chemotactic migration toward a hepatocyte growth factor (HGF) gradient and that the combination of HGF and CXCL12 promoted stronger migration of MSCs in vitro [27]. Because solid tumor tissues express and secrete growth factors, cytokines, and chemokines

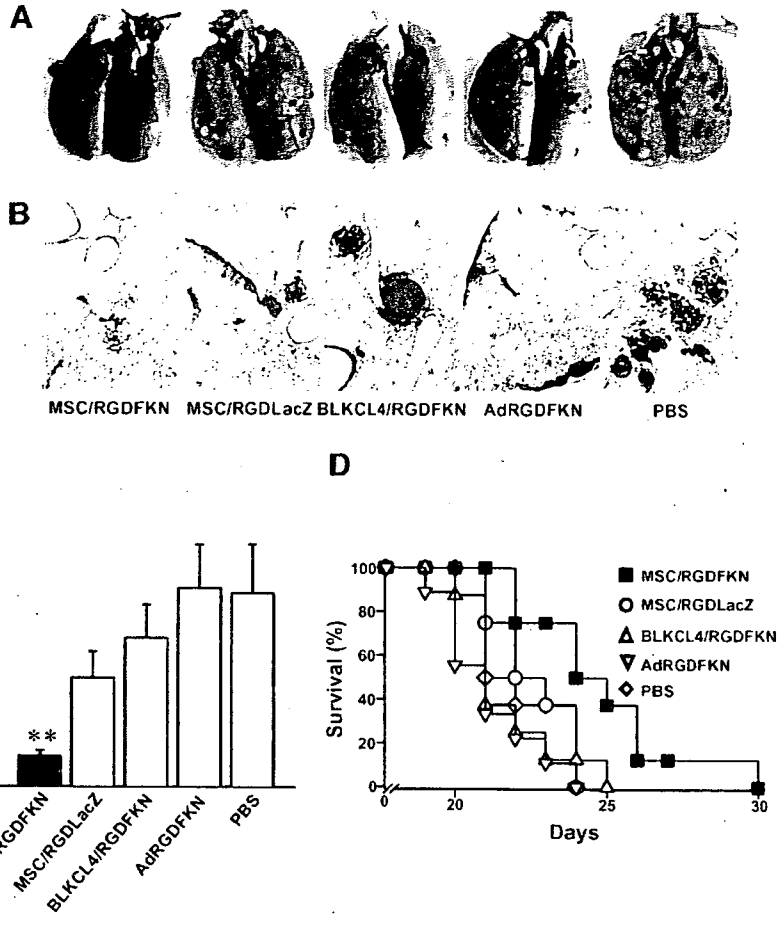

Figure 5. Inhibition of B16F10 lung metastases by single i.v. injection of MSCs/RGDFKN. B16F10 cells (5×10^5) were injected into the lateral tail vein of C57BL/6 mice (day 0). Five days later, mice were treated with i.v. injection of MSCs/RGDFKN (5×10^5 cells) or MSCs/RGDLacZ, i.v. injection of BLKCL4/RGDFKN, i.v. injection of AdRGDFKN virus (5×10^7 plaque-forming units), or PBS alone. **(A):** A representative macrograph of B16F10 pulmonary metastases on the lung surface filled with Bouin's fixative in each treatment group. **(B):** A representative micrograph of B16F10 metastatic lung tumors stained with H&E in each treatment group. **(C):** Numbers of pulmonary metastatic nodules in each treatment group. The data represent the mean ± SD of results from eight mice. **, $p < .01$. **(D):** Mice with established pulmonary metastases of B16F10 were treated as described above. ■, MSCs/RGDFKN; ○, MSCs/RGDLacZ; △, BLKCL4/RGDFKN; ▽, AdRGDFKN vector; ◇, PBS. Survival curves were drawn by the Kaplan-Meier method ($n = 8$ in each treatment group). Abbreviations: AdRGDFKN, adenoviral vector carrying fractalkine; PBS, phosphate-buffered saline; RGDFKN, AdRGD expressing fractalkine; RGDLacZ, AdRGD expressing *β-galactosidase reporter* gene LacZ.

(e.g., CXCL12 and HGF) similar to injured tissues, MSCs are likely to migrate to tumor tissues through these factors.

MSCs have been proposed for cell therapy and cell-based gene therapy because MSCs migrate to the site of tissue injury and differentiate into several types of cells. Although several vectors have been applied for gene transfer to MSCs, the low efficiency of infection remains a challenge [28]. Adenoviral vectors have been widely used for gene transfer because of their efficient gene transfer and high expression of transgenes. However, conventional adenoviral vectors cannot efficiently transduce genes to MSCs because MSCs poorly express CAR [29]. We have previously demonstrated that a modified adenoviral vector could efficiently transduce to MSCs. We generated a fiber-modified adenoviral vector that showed high expression of CX3CL1 on the cell surface, as well as the secreted form of CX3CL1 at 50 MOI [24]. In contrast, in other reports, MOIs of over 1,000 were required to express sufficient amounts of biological products from MSCs [14].

The successful treatments of multiple tumors by engineered MSCs have been reported by Studeny et al. [13, 14]. They treated multiple lung metastases of human tumors in SCID mice by i.v. injection of human MSCs expressing interferon-β and demonstrated the inhibition of tumor growth in the lung. They extended this therapeutic strategy to the treatment of intracranial human gliomas in nude mice by injection of human MSCs expressing interferon-β through the carotid artery [15]. Although our study also demonstrated successful treatment of multiple lung metastases by systemic administration of MSCs, we failed to treat metastases to other organs, such as subcutaneous tumors. This discrepancy may be attributed to the difference between human MSCs and mouse MSCs or the low number of migrated MSCs to induce sufficient antitumor effects [30]. Repeated injection of engineered MSCs can be a way to enhance the antitumor effects in other organs. These limitations in the effectiveness should be solved before clinical application.

Neural stem cells also display extensive tropism to gliomas after intravascular administration [31]. Glioblastoma in the rat brain was successfully treated by neural progenitor cells expressing interleukin-4 [32] or the prodrug activating enzyme cytosine deaminase [33]. Although the neural stem cells were obtained from the cortex of rat brain in these experiments, neural stem cell-like cells can be obtained from bone marrow. Genetically modified neural stem cell-like cells migrate to the tumor site and inhibit the growth of U87-MG glioblastoma [34]. Thus, neural progenitor cells derived from bone marrow could be useful for glioblastoma.

Several genes, including immunostimulatory genes and a suicide gene, have been applied for MSC-based cancer gene therapy [13, 32, 33]. We chose CX3CL1 gene for MSC gene therapy for multiple lung tumors because CX3CL1 induces both innate and adaptive immunity [21]. In this study, dominant infiltration of $CD8^+$ lymphocytes and NK cells was observed in the tumors treated by MSCs/RGDFKN. Depletion of NK cells or $CD8^+$ lymphocytes resulted in the complete disappearance of the antitumor effect by MSCs/RGDFKN, suggesting that the effects of MSCs/RGDFKN depend on both innate and adaptive immunity. Although we did not demonstrate in vitro cytotoxic effects by lymphocytes after MSCs/RGDFKN treatment, it is likely that CX3CL1 induced cytotoxic T lymphocytes as we showed previ-

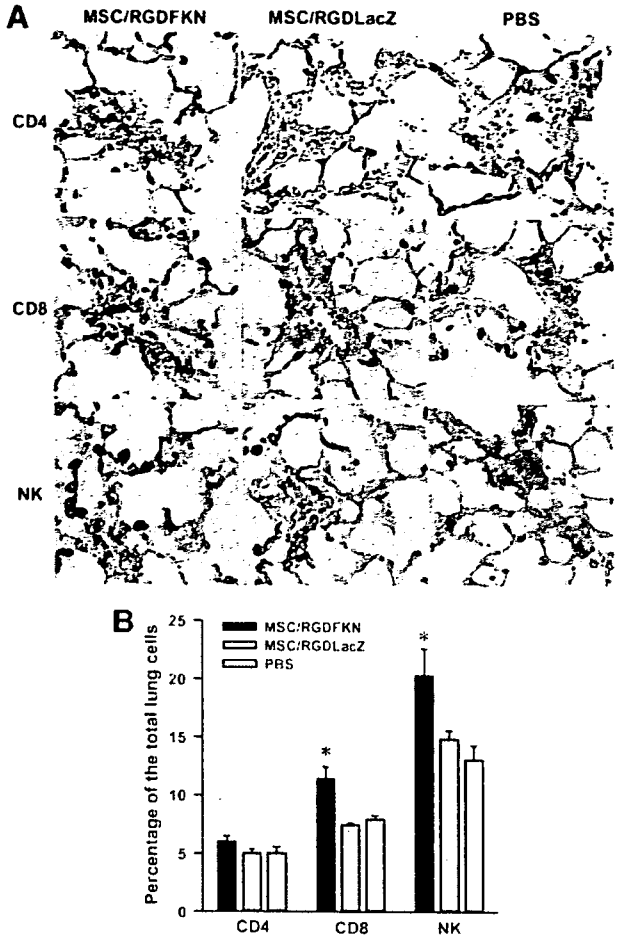

Figure 6. Infiltration of immune cells into the C26 lung tumors after MSCs/RGDFKN injection. BALB/c mice with C26 lung tumors were treated by i.v. injection of 5×10^5 of MSCs/RGDFKN, MSCs/RGD-LacZ, or PBS alone. The mice were sacrificed 3 days after treatment. **(A):** The lung tumors stained with anti-asialo GM1, anti-CD4, and anti-CD8 antibody (magnification, ×400). **(B):** Quantification of the numbers of NK, $CD4^+$, and $CD8^-$ cells in the lung with C26 tumors by fluorescence-activated cell sorting analysis. Data represent mean ± SD of five mice. *, $p < .05$. Abbreviations: NK, natural killer; PBS, phosphate-buffered saline; RGDFKN, AdRGD expressing fractalkine; RGDLacZ, AdRGD expressing *β-galactosidase reporter* gene LacZ.

ously [21]. All mice eventually died after MSCs/RGDFKN treatment due to incomplete eradication of pulmonary metastases. This incomplete eradication may be due to an insufficient number of migrated MSCs and/or evasion of tumor cells from antitumor immune response induced by CX3CL1.

We isolated and propagated mouse MSCs from bone marrow by their adherence to plastic and confirmed that these MSCs were capable of differentiating to adipocytes and osteoblasts. In several reports, CD45-positive cells were depleted from bone marrow cells before starting the culture for MSCs [35], because cultured adherent cells from bone marrow contain heterogeneous cell populations [36]. Although we did not deplete $CD45^+$ cells for isolating MSCs, we assume that the majority of these adherent cells would be MSCs because these cells could differentiate to multiple mesenchymal lineages.

In conclusion, we have demonstrated that mouse MSCs could be efficiently transduced by an adenoviral vector with the RGD motif. Systemic administration of MSCs could target multiple lung tumors and induce antitumor effects after tail vein injection. MSCs can serve as cellular vehicles to deliver biological agents, which exhibit antitumor effects against multiple lung tumors.

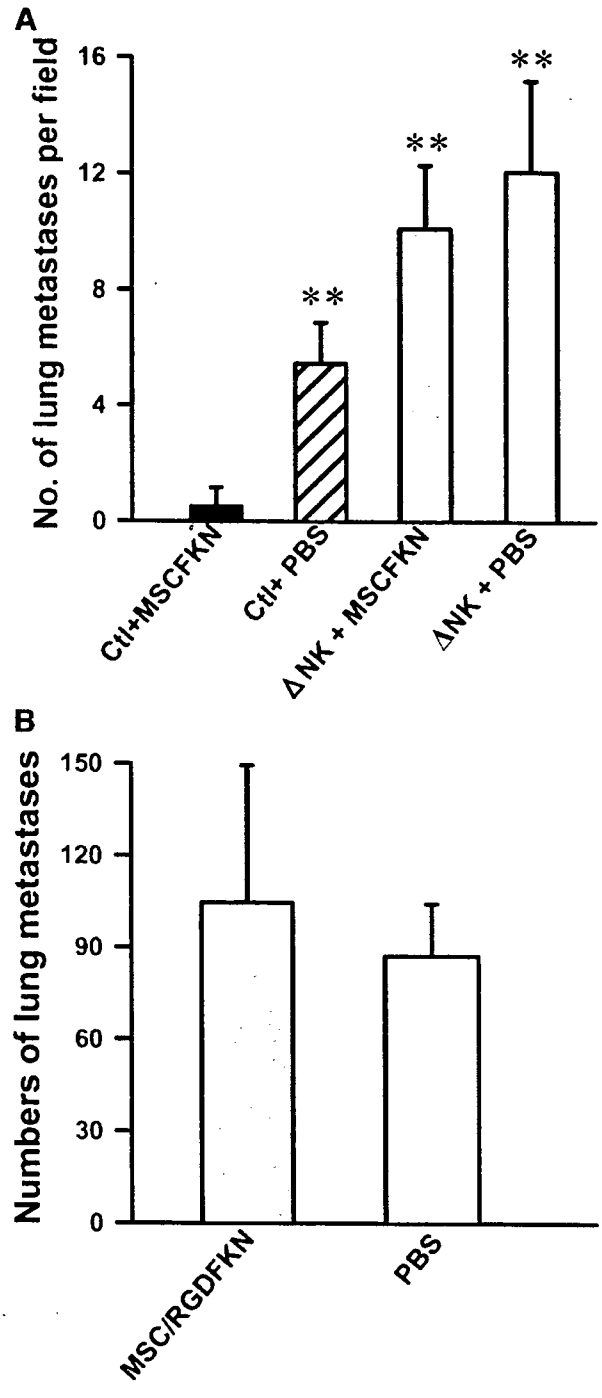

Figure 7. The role of NK cells and $CD8^+$ T-cells in the inhibition of lung metastases by MSCs/RGDFKN. **(A):** NK-depleted mice with pulmonary metastases of B16F10 were treated by i.v. injection of 5×10^5 MSCs/RGDFKN. IgG was injected as a Ctl for anti-asialo GM1 antibody. The metastatic nodules on the lung surface were counted. **(B):** $CD8^+$-deficient mice were also treated by MSCs/RGDFKN. The metastatic nodules on the lung surface were counted macroscopically. The data represent the mean ± SE of results ($n = 7$). **, $p < .01$. Abbreviations: Ctl, control; MSCFKN, MSC fractalkine; NK, natural killer; No., number; PBS, phosphate-buffered saline; RGDFKN, Ad-RGD expressing fractalkine.

ACKNOWLEDGMENTS

This work was supported in part by Grants-in-Aid for Scientific Research 16022206 and 16390232 from the Ministry of Education, Science, Sports, Culture, and Technology of Japan.

REFERENCES

1 Tahara H, Lotze MT, Robbins PD et al. IL-12 gene therapy using direct injection of tumors with genetically engineered autologous fibroblasts. Hum Gene Ther 1995;6:1607–1624.
2 Iwaguro H, Yamaguchi J, Kalka C et al. Endothelial progenitor cell vascular endothelial growth factor gene transfer for vascular regeneration. Circulation 2002;105:732–738.
3 Specht JM, Wang G, Do MT et al. Dendritic cells retrovirally transduced with a model antigen gene are therapeutically effective against established pulmonary metastases. J Exp Med 1997;186:1213–1221
4 Rosenberg SA, Yannelli JR, Yang JC et al. Treatment of patients with metastatic melanoma with autologous tumor-infiltrating lymphocytes and interleukin-2. J Natl Cancer Inst 1994;86:1159–1166.
5 Kasid A, Morecki S, Aebersold P et al. Human gene transfer: Characterization of human tumor-infiltrating lymphocytes as vehicles for retroviral-mediated gene transfer in man. Proc Natl Acad Sci USA 1990; 87:473–477.
6 Rosenberg SA, Aebersold P, Cornetta K et al. Gene transfer into humans—Immunotherapy of patients with advanced melanoma, using tumor-infiltrating lymphocytes modified by retroviral gene transduction. N Engl J Med 1990;323:570–578.
7 Colter DC, Class R, DiGirolamo CM et al. J Rapid expansion of recycling stem cells in cultures of plastic-adherent cells from human bone marrow. Proc Natl Acad Sci USA 2000;97:3213–3218.
8 Pittenger MF, Mackay AM, Beck SC et al. Multilineage potential of adult human mesenchymal stem cells. Science 1999;284:143–147.
9 Gojo S, Gojo N, Takeda Y et al. In vivo cardiovasculogenesis by direct injection of isolated adult mesenchymal stem cells. Exp Cell Res 2003; 288:51–59.
10 Sato Y, Araki H, Kato J et al. Human mesenchymal stem cells xenografted directly to rat liver are differentiated into human hepatocytes without fusion. Blood 2005;5;106:756–763.
11 Rojas M, Xu J, Woods CR et al. Bone marrow-derived mesenchymal stem cells in repair of the injured lung. Am J Respir Cell Mol Biol 2005;33:145–152.
12 Hung SC, Deng WP, Yang WK et al. Mesenchymal stem cell targeting of microscopic tumors and tumor stroma development monitored by noninvasive in vivo positron emission tomography imaging. Clin Cancer Res 2005;11:7749–7756.
13 Studeny M, Marini FC, Champlin RE et al. Bone marrow-derived mesenchymal stem cells as vehicles for interferon-beta delivery into tumors. Cancer Res 2002;62:3603–3608.
14 Studeny M, Marini FC, Dembinski JL et al. Mesenchymal stem cells: Potential precursors for tumor stroma and targeted-delivery vehicles for anticancer agents. J Natl Cancer Inst 2004;96:1593–1603.
15 Nakamizo A, Marini F, Amano T et al. Human bone marrow-derived mesenchymal stem cells in the treatment of gliomas. Cancer Res 2005; 65:3307–3318.
16 Pereboeva L, Komarova S, Mikheeva G et al. Approaches to utilize mesenchymal progenitor cells as cellular vehicles. STEM CELLS 2003; 21:389–404.
17 Tsuda H, Wada T, Ito Y et al. Efficient BMP2 gene transfer and bone formation of mesenchymal stem cells by a fiber-mutant adenoviral vector. Mol Ther 2003;7:354–365.
18 Bazan JF, Bacon KB, Hardiman G et al. A new class of membrane-bound chemokine with a CX3C motif. Nature 1997;385:640–644.

DISCLOSURE OF POTENTIAL CONFLICTS OF INTEREST

The authors indicate no potential conflicts of interest.

19 Rossi D, Zlotnik A. The biology of chemokines and their receptors. Annu Rev Immunol 2000;18:217–242.
20 Imai T, Hieshima K, Haskell C et al. Identification and molecular characterization of fractalkine receptor CX3CR1, which mediates both leukocyte migration and adhesion. Cell 1997;91:521–530.
21 Xin H, Kikuchi T, Andarini S et al. Antitumor immune response by CX3CL1 fractalkine gene transfer depends on both NK and T cells. Eur J Immunol 2005;35:1371–1380.
22 Arai F, Ohneda O, Miyamoto T et al. Mesenchymal stem cells in perichondrium express activated leukocyte cell adhesion molecule and participate in bone marrow formation. J Exp Med 2002;195:1549–1563.
23 Mizuguchi H, Koizumi N, Hosono T et al. A simplified system for constructing recombinant adenoviral vectors containing heterologous peptides in the HI loop of their fiber knob. Gene Ther 2001;8:730–735.
24 Gao JQ, Tsuda Y, Katayama K et al. Antitumor effect by interleukin-11 receptor alpha-locus chemokine/CCL27, introduced into tumor cells through a recombinant adenovirus vector. Cancer Res 2003;63: 4420–4425.
25 Wynn RF, Hart CA, Corradi-Perini C et al. A small proportion of mesenchymal stem cells strongly expresses functionally active CXCR4 receptor capable of promoting migration to bone marrow. Blood 2004; 104:2643–2645.
26 Sordi V, Malosio ML, Marchesi F et al. Bone marrow mesenchymal stem cells express a restricted set of functionally active chemokine receptors capable of promoting migration to pancreatic islets. Blood 2005;106: 419–427.
27 Son BR, Marquez-Curtis LA, Kucia M et al. Migration of bone marrow and cord blood mesenchymal stem cells in vitro is regulated by SDF-1-CXCR4 and HGF-c-met axes and involves matrix metalloproteinases. STEM CELLS 2006;24:1254–1264.
28 Mangi AA, Noiseux N, Kong D et al. Mesenchymal stem cells modified with Akt prevent remodeling and restore performance of infarcted hearts. Nat Med 2003;9:1195–1201.
29 Hung SC, Lu CY, Shyue SK et al. Lineage differentiation-associated loss of adenoviral susceptibility and coxsackie-adenovirus receptor expression in human mesenchymal stem cells. STEM CELLS 2004;22: 1321–1329.
30 Peister A, Mellad JA, Larson BL et al. Adult stem cells from bone marrow (MSCs) isolated from different strains if inbred mice vary in surface epitopes, rates of proliferation, and differentiation potential. Blood 2004;103:1662–1668.
31 Aboody KS, Brown A, Rainov NG et al. Neural stem cells display extensive tropism for pathology in adult brain: Evidence from intracranial gliomas. Proc Natl Acad Sci USA 2000;97:12846–12851.
32 Benedetti S, Pirola B, Pollo B et al. Gene therapy of experimental brain tumors using neural progenitor cells. Nat Med 2000;6:447–450.
33 Brown AB, Yang W, Schmidt NO et al. Intravascular delivery of neural stem cell lines to target intracranial and extracranial tumors of neural and non-neural origin. Hum Gene Ther 2003;14:1777–1785.
34 Lee J, Elkahloun AG, Messina SA et al. Cellular and genetic characterization of human adult bone marrow-derived neural stem-like cells: A potential antiglioma cellular vector. Cancer Res 2003;63:8877–8889.
35 Pevsner-Fischer M, Morad V, Cohen-Sfady M et al. Toll-like receptors and their ligands control mesenchymal stem cell functions. Blood 2007; 109:1422–1432.
36 Phinney DG, Kopen G, Isaacson RL et al. Plastic adherent stromal cells from the bone marrow of commonly used strains of inbred mice: Variations in yield, growth, and differentiation. J Cell Biochem 1999;72: 570–585.